

Age-related changes in the biochemical composition of the human aorta and their correlation with the delamination strength

Tomáš Suchý^{a,b,*}, Lukáš Horný^b, Monika Šupová^a, Tomáš Adámek^c, Alžběta Blanková^c, Margit Žaloudková^a, Martina Grajciarová^{d,e}, Olena Yakushko^d, Tereza Blassová^{d,e}, Martin Braun^a

^a Department of Composites and Carbon Materials, Institute of Rock Structure and Mechanics, Czech Academy of Sciences, 182 09 Prague 8, Czech Republic

^b Faculty of Mechanical Engineering, Czech Technical University in Prague, 160 00 Prague 6, Czech Republic

^c Department of Forensic Medicine and Toxicology, Regional Hospital Liberec, Husova 357/10, 460 63, Liberec, Czech Republic

^d Department of Histology and Embryology, Faculty of Medicine in Pilsen, Charles University, Czech Republic

^e Biomedical Center, Faculty of Medicine in Pilsen, Charles University, Czech Republic

* Correspondence: suchy@irms.cas.cz; Tel.: +420-777-608-280

Abstract (normally less than 200 words; must not exceed 250 words)

Various studies have correlated the mechanical properties of the aortic wall with its biochemical parameters and inner structure. Very few studies have addressed correlations with the cohesive properties, which are crucial for understanding fracture phenomena such as aortic dissection, i.e. a life-threatening process. Aimed at filling this gap, we conducted a comprehensive biochemical and histological analysis of human aortas (the ascending and descending thoracic and infrarenal abdominal aorta) from 34 cadavers obtained post-mortem during regular autopsies. The pentosidine, hydroxyproline and calcium contents, calcium/phosphorus molar ratio, degree of atherosclerosis, area fraction of elastin, collagen type I and III, alpha smooth muscle actin, vasa vasorum, vasa vasorum density, aortic wall thickness, thicknesses of the adventitia, media and intima were determined and correlated with the delamination forces in the longitudinal and circumferential directions of the vessel as determined from identical cadavers. The majority of the parameters determined did not indicate significant correlation with age, except for the calcium content and collagen maturation (enzymatic crosslinking). The main results concern differences between enzymatic and non-enzymatic crosslinking and those caused by the presence of atherosclerosis. The enzymatic crosslinking of collagen increased with age and was accompanied by a decrease in the delamination strength, while non-enzymatic crosslinking tended to decrease with age and was accompanied by an increase in the delamination strength. As the rate of calcification increased, the presence of atherosclerosis led to the formation of calcium phosphate plaques with higher solubility than the tissue without or with only mild signs of atherosclerosis.

Keywords: AGEs, Atherosclerosis, Calcification, Collagen maturation, Delamination, FTIR, Human aorta

1. Introduction

The wall of the aorta, the main artery in the human body, is characterized by a highly organized internal structure [1–5]. Its three layers differ in terms both of their function and composition. The tunica intima, i.e. the inner layer, is relatively thin and due to its sensitivity to mechanical stress constitutes the fundamental element in terms of the mechanobiological interaction that serves to maintain homeostasis [4]. The tunica media, the middle layer, consists of musculo-elastic fascicles that create concentric membranes that surround circumferentially oriented smooth muscle cells, and the whole structure is interlaced with a network of collagen fibers that lie between the membranes and create radially running connections [4–7]. The tunica adventitia, the outer layer, contains fibroblasts and

bundles of collagen fibers, and anchors the aorta to the surrounding tissue from which it is penetrated by nerves and vasa vasorum [1,4,5,8–12].

Since the number of elastic membranes varies along the length of the aorta, its biomechanical properties depend on the location [1,4,6,7,11]. In general, it can be stated that the aorta is anisotropic, nonlinear and viscoelastic [1,3,4,13–24]. The mechanical properties of the aorta, moreover, change with age [13–16,20–25]. Certain changes that occur over the human lifetime in the cardiovascular system can be attributed to aging that leads to the accumulation of DNA damage followed by changes in the cellular functions, which results in an overall decline in the circulation physiology [26,27]. Concerning arteries, however, from the clinical and biomechanical point of view, the consequences of aging are usually dominated by two pathologically and etiologically distinct processes that assume physiological significance over the time scale of decades, i.e. atherosclerosis and arteriosclerosis [28–31]. Both diseases lead to the gradual stiffening of the arteries, which correlates so strongly with age that it may be difficult to distinguish them from each other without the performance of a microstructural analysis [32,33].

Atherosclerosis is manifested by the formation of focal lesions, which, via several developmental stages, progresses from the accumulation of monocytes and macrophages, through the accumulation of lipids and molecules that accompany the inflammatory process, to the formation of calcium deposits in a form and concentration that significantly alters the mechanical properties of the vascular wall and restricts lumen cross-section [30,34–38]. From the etiological point of view, the development of atherosclerosis differs from that of arteriosclerosis, which can be described as the age-related accumulation of calcium that binds to elastin [39–41] and is followed by the fragmentation of the elastic membranes [42] that results in the transfer of the load-bearing capacity from the elastic component to the collagen network. Due to its impact on the tunica media, arteriosclerosis is sometimes referred to as medial elasto-calcinosis or Monckeberg sclerosis [28,30,32,33]. Unlike atherosclerosis, the clinical manifestation of which concerns primarily the restriction of the blood supply, arteriosclerosis exerts a clinical impact on blood pressure and the pattern and velocity of the pressure wave [29,34].

Enzymatic and non-enzymatic crosslinking, involving both collagen and elastic fibers, comprise further mechanisms that act to change the mechanical properties of the aorta [35–38]. One of the important differences between the two crosslinking processes concerns the fact that enzymatic crosslinking occurs primarily intra-molecularly and is essential for optimal tissue functioning [35,37,39,40]. Enzymatic crosslinks typically form between lysine and hydroxy-lysine at the N-/C-terminal, facilitated by lysyl oxidases and dehydration that form covalent bonds [35,41]. Non-enzymatic cross-linking associated with aging occurs both intra- and inter-molecularly; however, with concern to collagen it does not involve telopeptides [39,42–44]. Rather, in terms of tissue functioning, it leads to structural deleterious changes [39]. Non-enzymatic crosslinking acts predominantly via advanced glycation end products (AGEs) which arise via the Maillard reaction. AGEs-induced crosslinks restrict the compliance of extracellular matrix scleroproteins, which results in tissue stiffening [28,45–47]. Pentosidine (PEN) comprises one of the best chemically-defined representatives of the AGEs group [48–52].

Although studies that have investigated the impact of glycation on the tensile properties of the arterial wall suggest that elastin, in particular, is susceptible to glycation changes, and that arteries gradually stiffen and change the character of their viscoelastic response under such conditions [36,45,46,53–55], the situation is somewhat different with concern to the cohesive properties [56]. These properties play an essential role in the formation and propagation of cracks as in aortic dissection. Although diabetes has been found to be closely related to cardiovascular diseases, and non-enzymatic glycation is magnified in diabetic patients, statistical studies concerning the risk of aortic dissection and its complications suggest that diabetes lowers the risk of dissection [57–62]. This is in accordance with

the findings of a recent study by Wang et al. [56] that showed that glucose treatment increased the delamination strength. This suggests a somewhat peculiar contradiction between the effect of glycation on the bulk material properties and the cohesive properties, which, to the best of our knowledge, has not yet been explained. Thus, our study aims to contribute to the understanding of this topic.

Our previous study has focused primarily on site-specific differences in terms of the delamination strength of the thoracic ascending, thoracic descending and abdominal parts of the human aorta, and its correlation with age [16]. Various studies have correlated the mechanical properties of the aortic wall with its structural or biochemical parameters; however, only very few studies have addressed correlations with its cohesive properties [63]. Aimed at filling this gap, we conducted a comprehensive biochemical and histological analysis of human aortic samples obtained from 34 cadavers. In addition to assessing the calcium content and the calcium/phosphate molar ratio, as well as the degree of atherosclerosis, the study included the quantitative histology results from the assessment of the elastin, collagen and smooth muscle cell (SMC) contents and the thickness of the aortic wall and its layers. However, the main result concerns the determination of the enzymatic and non-enzymatic crosslinking, i.e. the degree of collagen maturation and the quantitative determination of the degree of AGEs based on the PEN content. All the results were subjected to a correlation analysis with respect to the age and the delamination strength as addressed in our previous study [16]. To the best of our knowledge, no study has been published to date that compares the degree of enzymatic and non-enzymatic crosslinking and the delamination strength of the human aorta.

2. Materials and methods

2.1 Human aortas

Samples of human aortas were obtained post-mortem during regular autopsies carried out at the Department of Forensic Medicine and Toxicology at the Regional Hospital, Liberec. The post-mortem use of human tissue for the purposes of our project was approved by the Ethical Committee of the Regional Hospital, Liberec (under project no. GA20-11186S). The cohort that provided the aortic specimens comprised 34 individuals; 24 men (28-86 years, average age 58.2 ± 16.4 years; mean \pm SD) and 10 women (age 33-78, average age 59.7 ± 14.3 years). The autopsy reports were the only medical records available to us. All the tissues were taken from Caucasian donors. The entire aorta was excised from the body for the purposes of the study. The aorta was subsequently divided into three parts according to its anatomical sections, i.e. the ascending thoracic aorta (AAs), the descending thoracic aorta (ADs) and the infrarenal portion of the abdominal aorta (AAb). The autopsies were not able to provide samples from all three parts of the aorta from all the donors in the amount required for the planned range of biochemical analyses; thus, the distribution in each group was as follows; AAs: 32, ADs: 33, AAb: 34. A pathologist with more than 25 years of experience subsequently performed the qualitative evaluation of the degree of atherosclerosis for each section. The sections were then quantified on a scale of 0 to 4 according to morphological features: 0 – intact artery and fatty streaks, 1 – fibro-fatty plaques, 2 – advanced plaques, 3 – calcified plaques, 4 – ruptured plaques [64]. Following the basic pathological evaluation, the specimens were transported to the laboratory. Samples in the form of strips were prepared in the laboratory and taken from the proximal section of the AAs and from the middle sections of the ADs and AAbs. The mechanical testing was performed on the same day as the autopsy. The samples intended for the biochemical analyses were frozen at -25°C and lyophilized (BenchTop 4KZL, VirTis, USA) or fixed in formalin for histology purposes. The samples were kept in cold storage ($4 - 6^{\circ}\text{C}$) prior to autopsy and during transport. The mean interval between death and freezing was 63 ± 26 hours (mean \pm SD).

2.2 HPLC analysis of AGEs

The amount of advanced glycation end products was determined by means of the high-performance liquid chromatography (HPLC) quantification of PEN. PEN comprises one of the best chemically defined covalent crosslinks. It remained stable even following the acid hydrolysis of the aortic samples; moreover, it contains intense fluorophore, which allows for very sensitive and selective detection by means of HPLC. The HPLC method is suitable for the analysis of AGEs directly within tissues and provides accurate and reproducible results for specific AGEs molecules in a similar way to fluorimetric tests or ELISA-based immunochemical kits, which are, however, suitable for their determination in body fluids [65–67]. The correlation of the results obtained via HPLC for the determination of PEN and the spectrometric method for measuring the integral fluorescence of all the AGEs had been previously verified [65,68].

Approx. 20 mg of lyophilized tissue was available for the AGEs analysis for each sample. The sample treatment procedures for the determination of PEN include acid hydrolysis (in an aliquot of 12 M HCl for 16 hours), purification and the preconcentration of tissue hydrolysates by means of solid phase extraction (SPE) using a Visiprep™ SPE Vacuum Manifold DL vacuum manifold extractor from Supelco (Bellefonte, PA, USA), followed by the vacuum evaporation of the excessive solvents and reconstitution in the mobile phase and, finally, injection into the HPLC system. SPE based on selective sorption within the cellulose/water/*n*-butanol/glacial acetic acid separation system was applied so as to concentrate and purify the hydrolysate fraction that contained PEN.

The method adopted, optimized and applied for the determination of PEN in our laboratory is based on the reversed phase HPLC separation procedure employing the programmable gradient flow of the mobile phase and sensitive fluorescence detection [50,69]. The analysis involved the use of the Shimadzu on-line PC controlled HPLC system (Kyoto, Japan) operated by Lab Solutions software (LC Solution-Version 1.25) consisting of a liquid chromatograph (model: LC 10ADvp) equipped with an autosampler, quaternary pump, column oven and fluorescence detector (set at 335/385 nm excitation/emission). Separation was performed using a CGC Separon SGX C18 compact glass column filled with spherical silica gel particles (diameter 5 µm), modified with the octadecyl group; dimensions of 150 x 3 mm (Tessek, Prague, Czech Republic); the mobile phase applied consisted of 0.02 M heptafluorobutyric acid, 0.01 M (NH₄)₂SO₄, and the linear gradient was given by varying the concentration of acetonitrile (12.5–25.0% acetonitrile over 20 minutes), the column temperature was 40°C, the flow rate was 0.5 ml/min and the time of one HPLC run lasted 30 min. (including the returning of the mobile phase composition to the initial conditions); an amount of 10 µl of the sample reconstituted in the mobile phase was injected into the HPLC column. Injection was repeated three times (*n*=3) for each of the reconstituted samples. Following the peak area evaluation, the external standard method (calibration curve) was used to quantify the PEN, and the measured data was statistically evaluated. The pure pentosidine standard was purchased from Cayman Chemical (Ann Arbor, MI, USA).

2.3 Hydroxyproline determination

The hydroxyproline (HYP) content (expressed in terms of the weight amount of the dry aortic tissue), which can be taken as a direct biochemical marker of the collagen content, was determined according to the ISO 3496:1994(E) standard, Meat and Meat products – Determination of the Hydroxyproline Content. Approximately 5 mg of lyophilized tissue was used for the HYP analysis for each sample (*n*=3). The sample hydrolysates were oxidized using chloramine B. Following the quantitative reaction with *p*-dimethyldiaminobenzaldehyde, the HYP content in the hydrolysate was spectrophotometrically detected at 558 nm using a UV–Visible UV 530 spectrometer (Unicam Instruments, Cambridge, Great Britain). The collagen content in the tissues can be determined assuming an approx. 14% content of hydroxyproline in pure collagen [45].

2.4 Fourier Transform Infrared analysis

Fourier Transform Infrared (FTIR) spectroscopy allows for the evaluation of changes in the secondary structure of collagen and elastin molecules [70–73]. These changes may originate from additional age-associated crosslinking or interaction with calcium deposits. The FTIR spectra were measured using an iS50 (Thermo Nicolet Instruments Co., Madison, WI, USA) spectrometer via the attenuated total reflection (ATR) method. Dried samples were placed on the surface of the diamond crystal and compressed using a thrust screw. The area of the scanned spot on the diamond crystal was 7 mm². Infrared radiation was then emitted into the sample, averaging 64 scans with a resolution of 4 cm⁻¹ in the middle infrared range of 4000–400 cm⁻¹. The penetration depth into the sample surface was in the order of units of μm (i.e. approx. 3 μm at 1500 cm⁻¹ and approx. 10 μm at 400 cm⁻¹). The spectra obtained were processed using OMNIC Software 2019.

The protein FTIR spectra contain 5 amidic bands including N–H stretching at ~3300 cm⁻¹ for amide A, and amide B at ~3070 cm⁻¹, which represents the N–H bonds in the secondary amides together with C–H stretching in the sp² hybridization. The amide I bands (~1650 cm⁻¹) originate from C=O stretching vibrations coupled with N–H bending vibrations. The amide II bands (~1550 cm⁻¹) arise from N–H bending vibrations coupled with C–N stretching vibrations [74,75]. Finally, the FTIR spectra of collagen also evince a quartet of bands at ~1205, 1240, 1280 (amide III) and 1340 cm⁻¹ [76,77]. The FTIR spectra can be employed as a tool for the assessment of the maturation of collagen. The amide I region (~1650 cm⁻¹) can be deconvoluted into several distinct bands that describe the various types of secondary structures in collagen and elastin [78,79]. Of the various underlying bands that make up the amide I spectral peak, two are of particular interest in terms of the study of the maturity of collagen: 1660 and 1690 cm⁻¹. With concern to our study, the maturity of collagen was calculated as the ratio of the 1660/1690 sub-bands that are assigned to the mature and immature collagen crosslinks [80], respectively, that are present naturally in collagen and which increase with age [81,82].

2.5 Determination of the total Ca concentration

The total calcium concentration (expressed in terms of the weight amount of the dry aortic tissue) was determined applying atomic absorption spectroscopy (Varian AA 240, Agilent Technologies Inc., Santa Clara, CA) using the titration method. Approx. 5 mg of lyophilized tissue was available for the Ca analysis for each sample ($n=2$).

2.6 SEM and EDS analysis

Energy dispersive X-ray spectroscopy (EDS) using an Octane Elite SDDs (Ametek, USA) EDS detector on a STEM Apreo S LoVac scanning electron microscope (Thermo Fisher Scientific, USA) was applied for the chemical characterisation of the aortic tissue, particularly the assessment of the calcium/phosphorus (Ca/P) ratio. The contents of elemental Ca and P and the Ca/P weight ratio were analysed in order to detect changes in the calcification of the aortic tissue by both the different parts of the aorta and the donors. An EDS map was captured on each cross-section at a suitable magnification aimed at characterizing the inhomogeneity of the Ca/P distribution. The suitability of the magnification varied depending on the wall thickness of the aorta from each cadaver and was adjusted so as to capture the EDS map of the entire aortic wall cross-section thickness at the maximum possible resolution. Examples of EDS mapping are provided in Figures S1 and S2 in the Supplement.

2.7 Histological quantitative analysis

The stereological quantification was performed on the aortic samples obtained from the same donors ($n=27$) as in the case of the biochemical, structural and mechanical analysis, with the exception of 6 male ($n=18$) and 1 female ($n=9$) donors due to the insufficient quantities of the samples. All the aortic segments intended for the histological analysis were stored in a 10% neutral buffered formalin solution immediately following removal. The fixed aortic samples were dehydrated in ethanol, embedded in paraffin blocks and cut transversely into 5 μm-thick sections. The sections were deparaffinized,

rehydrated and stained applying a combination of four histological staining methods and two immunohistochemical reactions so as to allow for the visualization of the microscopic structures of the aorta wall. See Table 1 for a detailed description.

Table 1. Histological and immunohistochemical staining methods.

Staining methods	Purpose and visualization of the aortic wall components
Hematoxylin-eosin (Merc, C.I. 75290)	Overall morphology
Verhoeff's hematoxylin and green trichrome (Diapath, Italy, 2020)	Overall morphology, differentiation of connective tissue and smooth muscle
Orcein (Diapath, Italy, 2020)	Elastic fibers and elastic membranes
Direct red 80 (Sigma-Aldrich, Merc corp., USA, 2020)	Type I (yellow-red color) and type III collagen (green color) in polarized light
Immunohistochemistry with antibody anti-alpha smooth muscle actin (Clone 1A4, RTU dilution, Ventana, Roche Holding AG, USA)	Vascular alpha smooth muscle actin
Immunohistochemistry with antibody anti-CD31 (Clone JC70, RTU dilution, Cell Marque, Sigma-Aldrich, USA)	Endothelium of the vasa vasorum

Six microphotographs, as shown in Figure 1A, were employed to evaluate the area fractions of elastin, type I collagen, type III collagen, alpha smooth muscle actin and vasa vasorum, as well as the density of vasa vasorum in the tunica media using a 40x objective (Olympus Optical Co., Ltd., Tokyo, Japan). The microphotographs were determined via the systematic and uniform sampling procedure [10,83]. Sampling was performed for each of the 78 vascular segments examined (it was not possible to histologically process 3 segments from the total number of 81), thus resulting in a total of 1,872 microphotographs (78 vascular segments x 4 staining methods x 6 microphotographs). The digitized regions of the slides were utilized for the quantitative evaluation of the thicknesses of the tunica intima, media and adventitia, as well as for the qualitative assessment of the atherosclerotic changes in the human aorta applying the Olympus VS200 scanning system (Olympus Optical Co. Ltd., Tokyo, Japan), see Figure 1B.

The area fractions of elastin, type I collagen, type III collagen, alpha smooth muscle actin and vasa vasorum in the tunica media were evaluated employing a stereological point grid and the Cavalieri principle (Figure 2 A-D) [84] as described in previous studies [85–87]. The area fraction was quantified as the ratios of the structures of interest and the reference area. At least 150-point grid intersections with the structures of interest were considered [88]. The density of the vascular profiles was estimated using an unbiased counting frame (Figure 2E) [89–91]. The vascular density was calculated as the number of vasa vasorum per reference area. The stereological quantifications of the area fractions and density were performed using Ellipse software (ViDito, Košice, Slovakia). The thicknesses of the remodeled tunica intima, media and adventitia were quantified as the average value of four linear probe measurements (Figure 2F). The remodeled intima was considered to be the connective tissue layer from the endothelial cell lining to the internal elastic membrane or border, through which vascular SMCs migrated from the underlying media. This layer also contained accumulations of extracellular lipids and fat-laden foamy macrophages. The thickness of the outer layer of adventitial loose connective tissue was affected by the anatomical preparation process, therefore we considered only the dense connective tissue of the adventitia [11]. The scans obtained by the Olympus VS200 scanning system (Olympus, Japan) were utilized for the quantitative evaluation of the thickness; the scans were quantified using OlyVIA software (Olympus, Tokyo, Japan). See the summary of the histological procedures shown in Table 2.

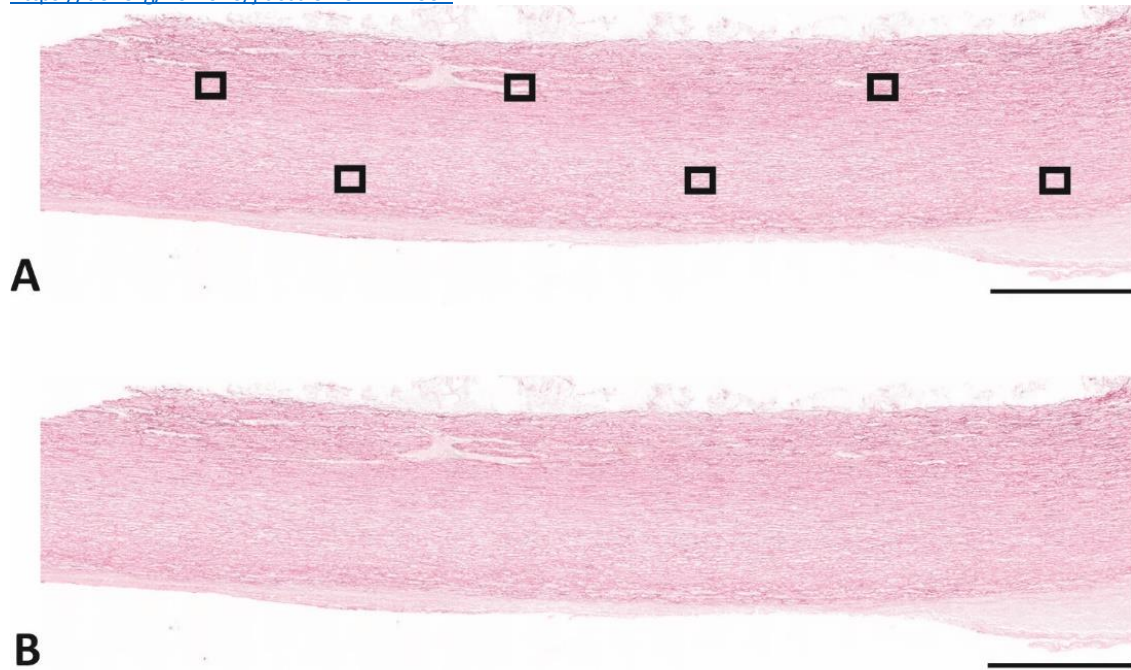


Figure 1. Systematic uniform sampling of the human aorta. **A** – Six microphotographs (as indicated by the black rectangles) were employed to evaluate the area fractions of elastin, type I collagen, type III collagen, total collagen, alpha smooth muscle actin and vasa vasorum, as well as the density of vasa vasorum in the tunica media using a 40x objective. **B** – Scans covering the entire region of the human aorta were used to assess the thicknesses of the tunica intima, media and adventitia, as well as the degree of atherosclerosis. Scale bars 1 mm (A, B).

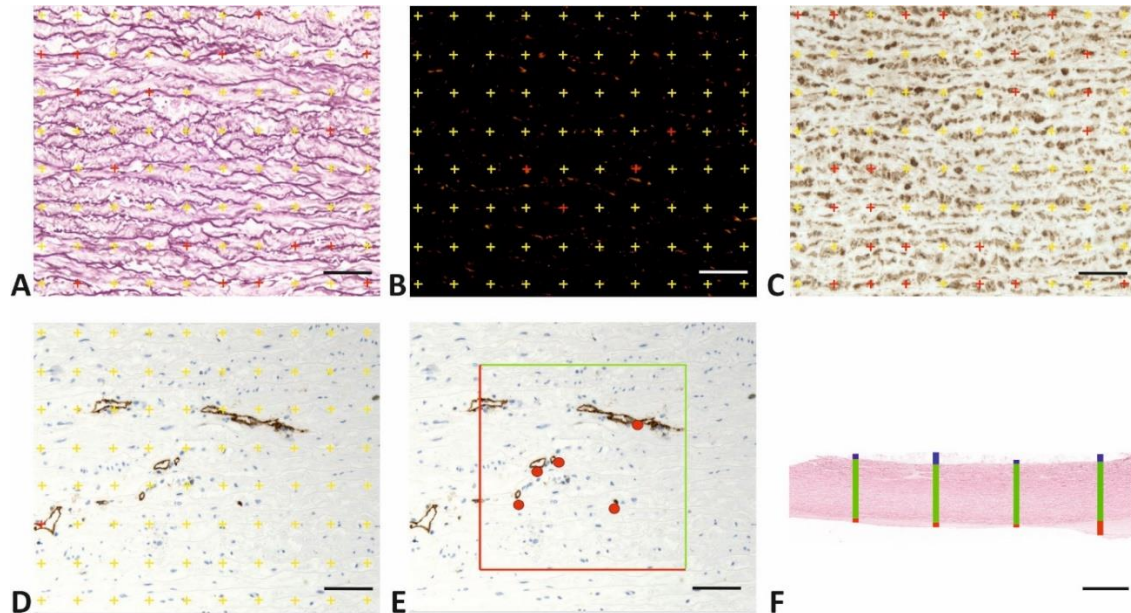


Figure 2. Stereological quantification of the microscopic structures and thicknesses of the aorta segments. **A** stereological point grid and the Cavalieri principle were used to quantify the area fractions of elastin (**A**), type I (yellow-red color) and III collagen (green color) (**B**), alpha smooth muscle actin (**C**), vasa vasorum (**D**). Unbiased counting frames were used to evaluate the density of the vasa vasorum (**E**). The thicknesses of the intima (red), media (green) and adventitia (blue) were evaluated as the average value of four linear probe measurements (**F**). Scale bars 50 μ m (A - E), 1 mm (F).

Table 2. Quantitative histological parameters, reference area, objective and number of microphotographs.

Quantitative parameter abbreviation and units	Reference area	Objective used	Micrographs taken
A _A (elastin, media) [-]	The area fraction of elastin fibers and membranes within the tunica media.	40x	6
A _A (type I collagen, media) [-]	The area fraction of type I collagen (yellow-red color) within the tunica media	40x	6
A _A (type III collagen, media) [-]	The area fraction of type III collagen (green color) within the tunica media	40x	6
A _A (actin, media) [-]	The area fraction of alpha smooth muscle actin within the tunica media	40x	6
A _A (vasa vasorum, media) [-]	The area fraction of vasa vasorum within the tunica media	40x	6
Q _A (vasa vasorum, media) [mm ⁻²]	The density of vasa vasorum within the tunica media	40x	6
Thickness [μm]	The thicknesses of the tunica intima, media and adventitia	20x	4 measurements

2.8 Determination of the delamination strength

A detailed description of the peeling experiments employed to investigate the delamination strength of the human aorta can be found in our previous study [16]. In contrast to the biochemical analyses, the samples were not exposed to any special physical or chemical treatment prior to the biomechanical experiments. Briefly, rectangular samples (approx. 8 × 60 mm) were cut from each aortic segment and aligned with both the longitudinal (L) and circumferential (C) directions of the vessel. An incision was made with a scalpel into the medial layer to provide for initial separation, which was then extended to approx. 3 cm in length. The arms of the T-shaped samples were used for the mounting of the samples to the clamps of the experimental tensile testing machine (Zwick/Roell, Messphysik). Both the delamination force necessary to increase the tear length and the tear length itself were recorded. The delamination strength S_d was considered as the ratio of the recorded force to the reference width of the samples. The S_d value obtained for a single specimen represented the median delamination strength found at a delamination length of 20 mm. The resulting S_d value used in the correlation analysis comprised the average of the four samples.

Our 3-year study included subjecting 661 aortic strips obtained from 46 cadavers to peeling experiments [16]. Of this number, a total of 544 strips were included in the correlation analysis of the cohesive properties and the biochemical and histological parameters, which were distributed as follows: 32 × 4 AAs, 28 × 4 ADs, and 34 × 4 AAbs (cadavers × strips). The results of the experiments showed that the delamination strength was insensitive to the loading rate; rather, it differed significantly according to the anatomical site on the aorta (AAs, ADs, AAb) and the orientation of the specimen L vs. C. A study by Horný et al. [16] performed a correlation analysis with respect to the length of the post-mortem interval, which revealed that the results were insensitive to the length of the post-mortem interval that applied in our study. Particular attention was devoted to the correlation of the delamination strength with age, which indicated a significant decrease in this respect [16]. In contrast to Horný et al. [16], this study also presents the results of the correlation with atherosclerosis, the histological structure, collagen maturation and other biochemical indices, which represent an assessment from the perspective of the internal structure of the vessel wall.

2.9 Statistical analysis

Part of the statistical analysis was performed in GraphPad Prism software (ver. 10.0.2 (232), GraphPad Software, San Diego, CA, USA). The normality of the data was verified applying the Shapiro-Wilk test and the construction of Q-Q plots. The homoscedasticity was verified applying the Bartlett and Brown-

Forsythe tests. Non-parametric analysis was employed since the assumption of normality or homoscedasticity was violated. The Kruskal-Wallis test was performed with a subsequent post hoc test based on the Dunn test (correction for multiple comparison). In the case of two-sample comparisons, the two-tailed Dunn test (without correction) was applied. Statistical significance was accepted at $p \leq 0.05$. The effect sizes were calculated as nonparametric rank-biserial correlation coefficients [92] which can be interpreted in the same way as the Pearson's correlation coefficient, i.e. small effect (0.1 - 0.3), medium effect (0.3 - 0.5) and large effect (0.5 - 1.0). This part of the statistical analysis was performed in JASP (ver. 0.17.2.1, JASP Team 2023, University of Amsterdam, Netherlands). Box-plots with Tukey intervals (whiskers) were employed for the graphical presentation of the data. The potential correlation of the biochemical and histological parameters with age and the delamination strength were determined by means of calculating the nonparametric Spearman correlation coefficients (without assumptions of the Gaussian distribution) with a two-tailed p value ($p \leq 0.05$ rejects the supposition that the correlation is due to random sampling).

3. Results

3.1 Biochemical and histological analyses

A summary of the results of all the biochemical and histological analyses performed for the three aortic locations is provided in Figure 3. No differences were detected in the PEN content between the AAs, ADs and AAb in the analysed tissues provided by the donors for our study purposes - it ranged from 30.7 to 43.9 pmol.g⁻¹ (median) per weight of the dried sample. The hydroxyproline content was highest in the AAb (3.6 wt%) and differed significantly from the content in both the ADs and the AAs (both 3.1 wt%), although the effect size was medium. The collagen maturity, determined as the ratio of the 1660/1690 sub-band areas, did not differ between the aortic sections (2.6 - 2.9), nor did the Ca content (0.46 - 0.79 wt%) or the molar Ca/P ratio (1.46 - 1.62). The histological analysis, however, revealed significant differences between the studied anatomical locations for the total thickness of the aortic wall (AAs: 2.08 - 2.61 mm, ADs: 1.52 - 1.87 mm, AAb: 1.85 - 2.24 mm; interquartile range (IQR)), thickness of the adventitia (AAs: 0.42 - 0.92 mm, ADs: 0.34 - 0.59 mm, AAb: 0.43 - 0.98 mm; IQR), thickness of the media (AAs: 1.27 - 1.75 mm, ADs: 0.94 - 1.19 mm, AAb: 0.70 - 0.95 mm; IQR), and thickness of the intima (AAs: 0.05 - 0.14 mm, ADs: 0.11 - 0.25, AAb: 0.25 - 0.45 mm; IQR). In all these cases, the effect size was found to be medium or large. In the case of actin, the highest area fraction was detected for the AAb (AAs: 0.20 - 0.27, ADs: 0.24 - 0.29, AAb: 0.25 - 0.39; IQR), whereas concerning elastin, the AAb evinced the lowest area fraction (AAs: 0.38 - 0.49, ADs: 0.39 - 0.48, AAb: 0.30 - 0.40; IQR); images are shown in Figure 4.

The quantitative biochemical and histological results obtained were further divided into groups according to the degree of atherosclerosis. None of the samples exhibited grade 4 atherosclerosis (ruptured plaques). Since the number of samples was too low to be able to adequately cover the remaining four stages of atherosclerosis, the samples were pooled into two groups. The first group, i.e. without, or with only mild indications of atherosclerosis (without or with mild signs of atherosclerosis; H) consisted of tissues that were qualitatively rated as intact artery, with fatty streaks or fibro-fatty plaques. The second group (with atherosclerosis; A) comprised the tissues in which calcified plaques were detected. The merging of groups 0 and 1 represented a certain degree of simplification; it was assumed that the pathological changes in group 1 had not yet significantly affected the hemodynamic and biomechanical properties of the arterial wall [93].

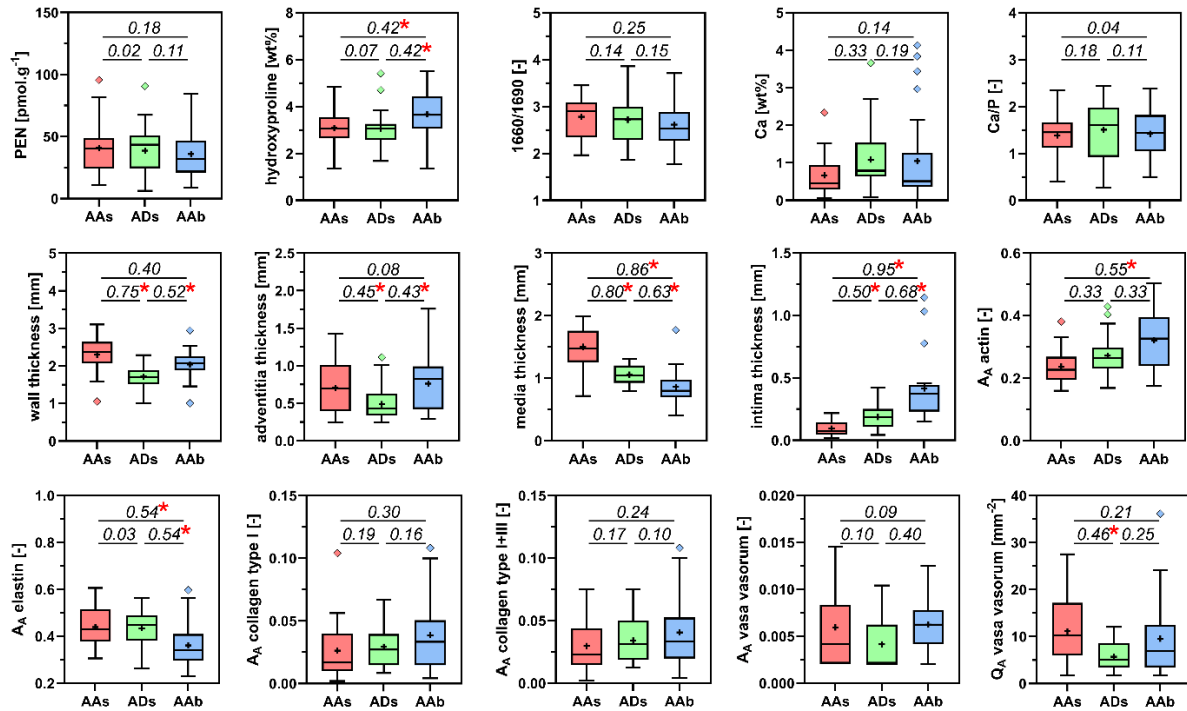


Figure 3. Biochemical and structural properties of the studied aortic segments. Pairs with p-values of <0.05 (the Dunn nonparametric test, $n=(20-32)$) are marked with “*”. The effect size is indicated by the rank-biserial correlation coefficients.

Figure 5 shows the results of the biochemical and histological analyses after the samples were classified according to atherosclerosis. Interestingly, the presence of atherosclerosis did not appear to be an important factor in terms of the values of the variables (PEN, hydroxyproline, collagen maturity, Ca, Ca/P, wall thickness, actin, elastin and collagen contents) studied in our sample (Figure 5). The aortic samples with atherosclerosis evinced differences that represented only small effect sizes compared to the healthy samples and those that showed mild signs of atherosclerosis. This finding, and the fact that the differences were not statistically significant, was undoubtedly influenced by the relatively high variance in the data obtained. When we focused on the differences with the predomination of the medium effect size in all three aortic segments, the differences between groups H and A related mainly to the structural parameters of the intima thickness and the area fraction of collagen types I+III. With the exception of the increase in the intima thickness (median 51-95%, medium or large effect size), the trend for the collagen I+III area fraction differed across the 3 sections of the aorta (AAs: -75%, ADs: -33%, AAb: +65%; medium effect size).

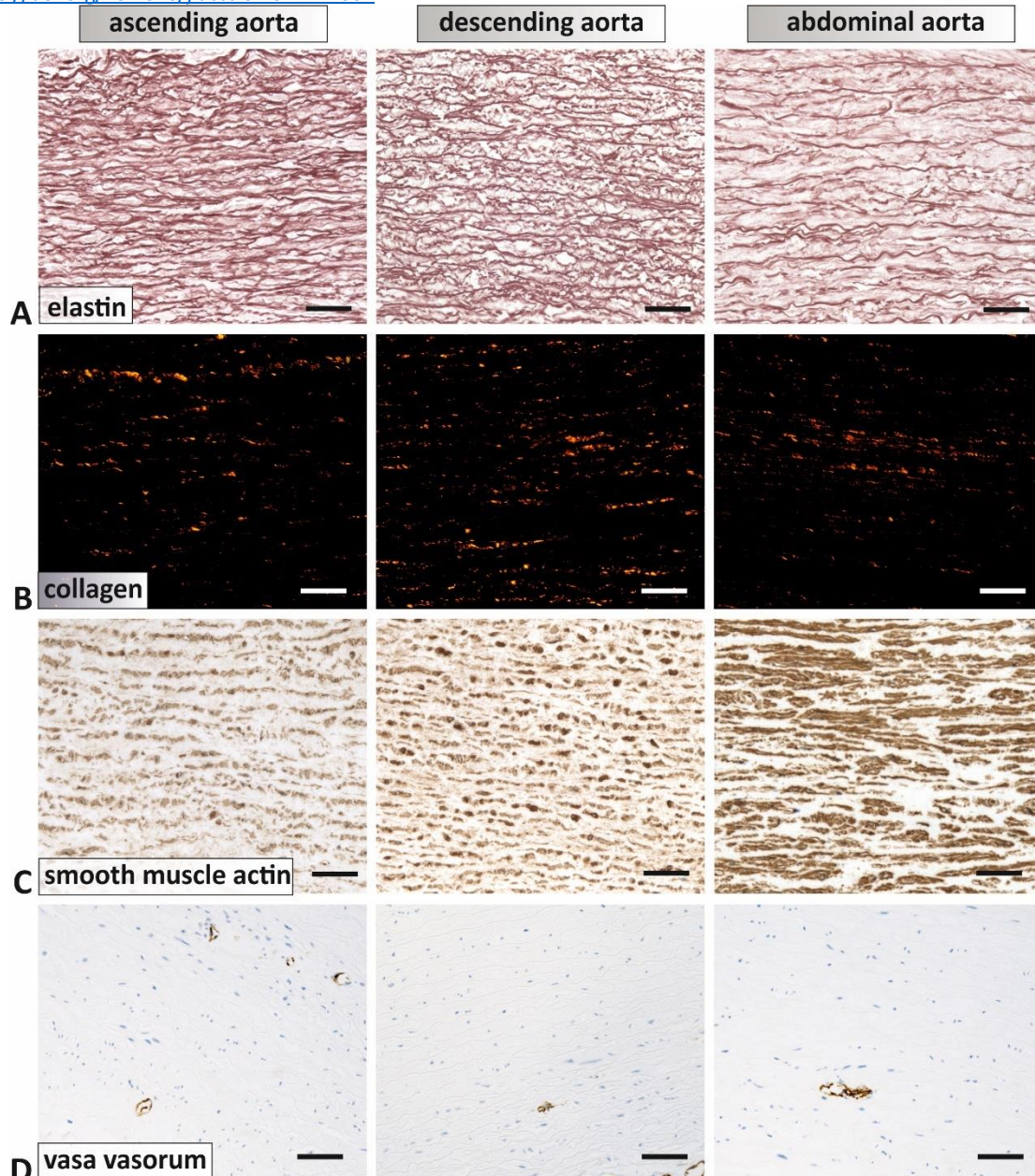


Figure 4. Comparison of the elastin, type I collagen, vascular alpha smooth muscle actin and vasa vasorum in the tunica media between the ascending, thoracic and abdominal parts of the aorta. **A** – The ascending aorta evinced a higher fraction of elastin than the abdominal aorta (the Dunn nonparametric test). The elastic fibers and membranes were stained using Orcein. **B** – All the aorta segments had the same fraction of collagen. Type I collagen (yellow and red) was visualized by means of Direct red 80 and viewed under polarized light. **C** – The abdominal aorta had a higher fraction of alpha smooth muscle actin than the ascending aorta. The alpha smooth muscle actin positive cells were stained using anti-alpha smooth muscle actin. **D** – The vasa vasorum fraction was the same in all the aorta segments. The endothelial cells of the vasa vasorum were stained using anti- CD31. Scale bar 50 μ m (A-D).

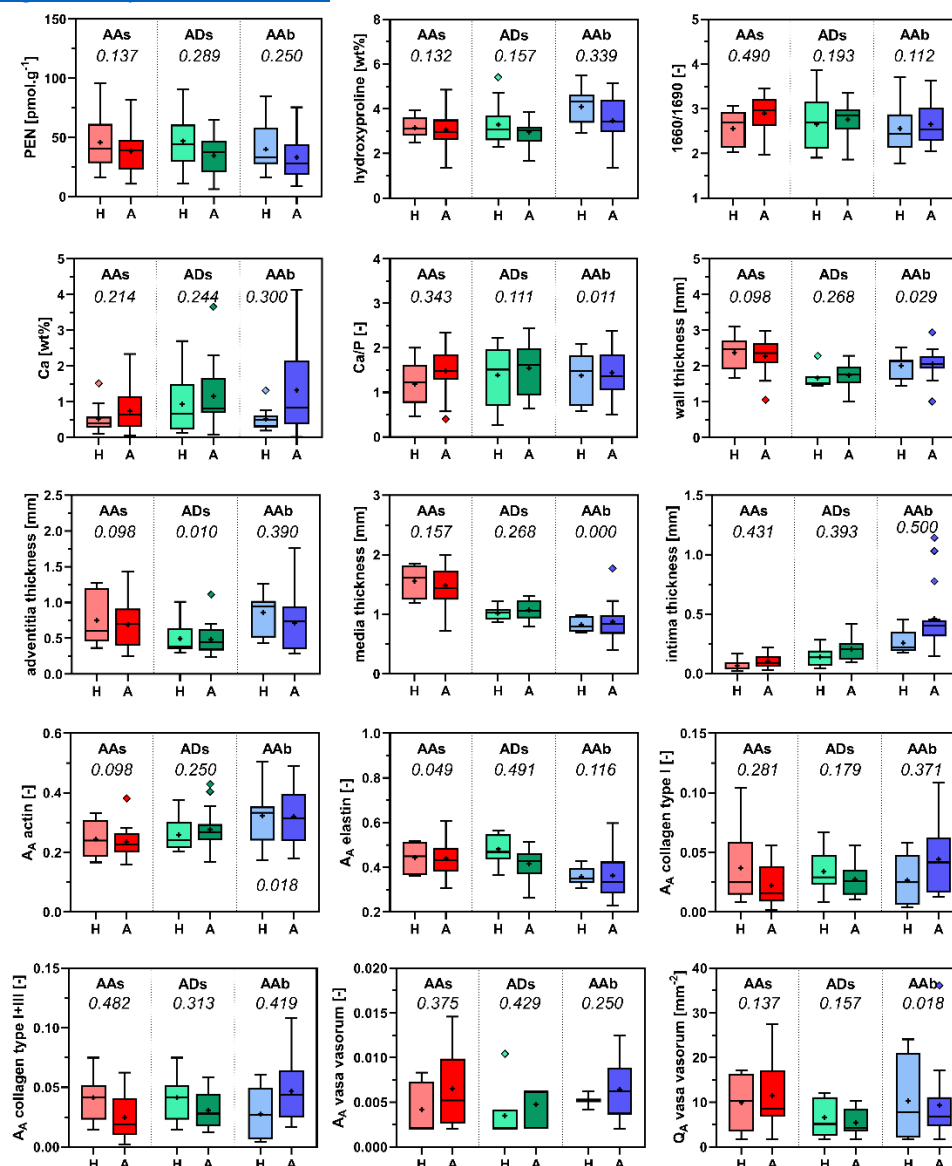


Figure 5. Biochemical and structural properties of the studied aortic segments. H indicates the samples without or with mild signs of atherosclerosis and A indicates the samples with atherosclerosis. The pairs with p-values of <0.05 (the Dunn nonparametric test, $n=(2-23)$) are marked with “*”. The effect size is indicated by the rank-biserial correlation coefficients.

3.2 Fourier Transform Infrared analysis

FTIR analysis was employed both for the study of the collagen maturation (1660/1690 in Figure 5) and to compare the samples with respect to their biochemical composition. An example of the difference between the FTIR spectra of a 33-year-old woman and a 76-year-old man is provided in Figure 6. The red spectrum (female, 33 years) contains only the amide bands of collagen and elastin. Another spectral region, the so-called carbohydrate region ($960-1140\text{ cm}^{-1}$), is composed of several underlying bands that refer to non-collagenous proteins, carbohydrate and proteoglycan [94]. In contrast, the dark blue spectrum observed in Figure 6 (male, 76 years) refers to the 1740 and 1165 and 720 cm^{-1} bands typical for aliphatic esters – lipids (pink rectangle). The bands at 2925 cm^{-1} (asymmetric stretching vibrations of CH_2) [76] provide further evidence of the existence of lipids. In addition to lipids, bands of cholesterol (yellow triangle) are also present. The blue spectrum also contains a band of phosphate anions (dark green circles) in two of the spectral regions, i.e. $1000-1100$ and $550-620\text{ cm}^{-1}$ typical for apatite calcification. The presence of lipids, apatite and cholesterol in the spectrum of

the 76-year-old man provides evidence of age-related changes in the biochemical composition of the aorta.

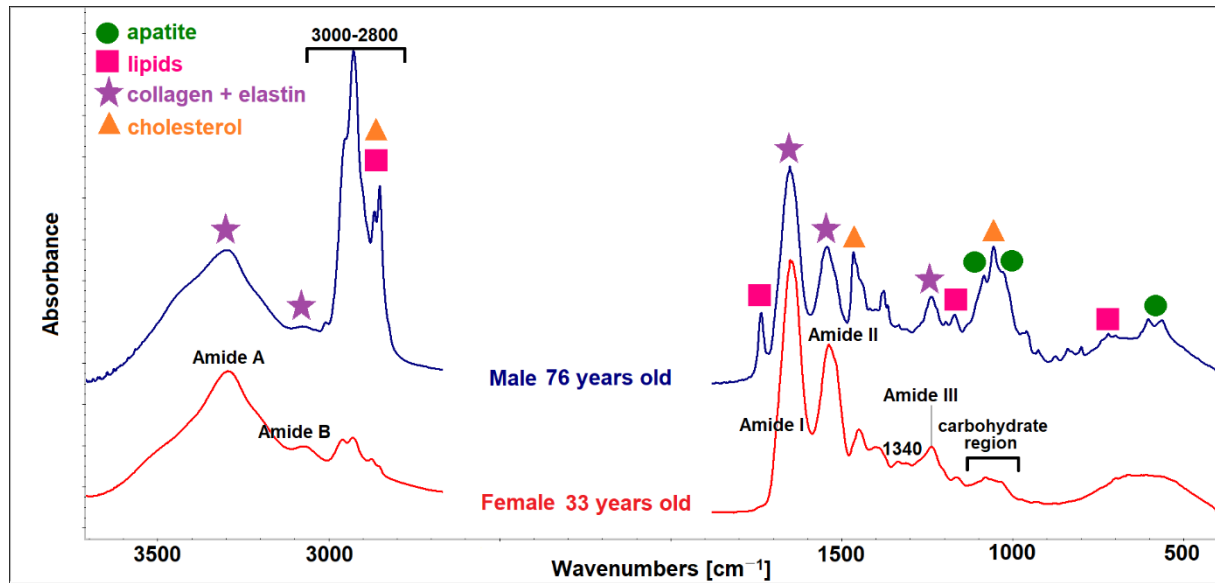


Figure 6. Comparison of the ATR-FTIR spectra of the AAb determined for a 33-year-old female (bottom, red spectrum) with a 76-year-old male (top, dark blue).

3.3 Correlation with age

The results of the correlation analysis showed that there was strong correlation in the sample between age and the collagen maturity, and age and the calcium content in all three anatomical locations (Figure 7). These correlations were significant and positive ($p < 0.05$; for a detailed summary of the Spearman rank correlation coefficients, see Table S1 in the Supplement). This demonstrated that collagen maturation increases with age, as does the calcium content. When the data was pooled into groups H (no or moderate atherosclerosis) and A (significant atherosclerosis), the correlations with age were less conclusive (Table S1). Positive and statistically significant correlations were also further observed in the group with atherosclerosis; however, concerning the non-atherosclerosis group, in no cases were they statistically significant. However, this was probably influenced by the small sample size ($n=9-11$) and the outlying points. The tendency concerning the determined PEN content was also of interest, i.e. a decreasing trend was observed with age (Figure 7). Although the correlation was not statistically significant, the observed trend indicates that the content of non-enzymatic crosslinks does not increase with age. The other biochemical and histological parameters did not evince a clear significant correlation with age (Table S1).

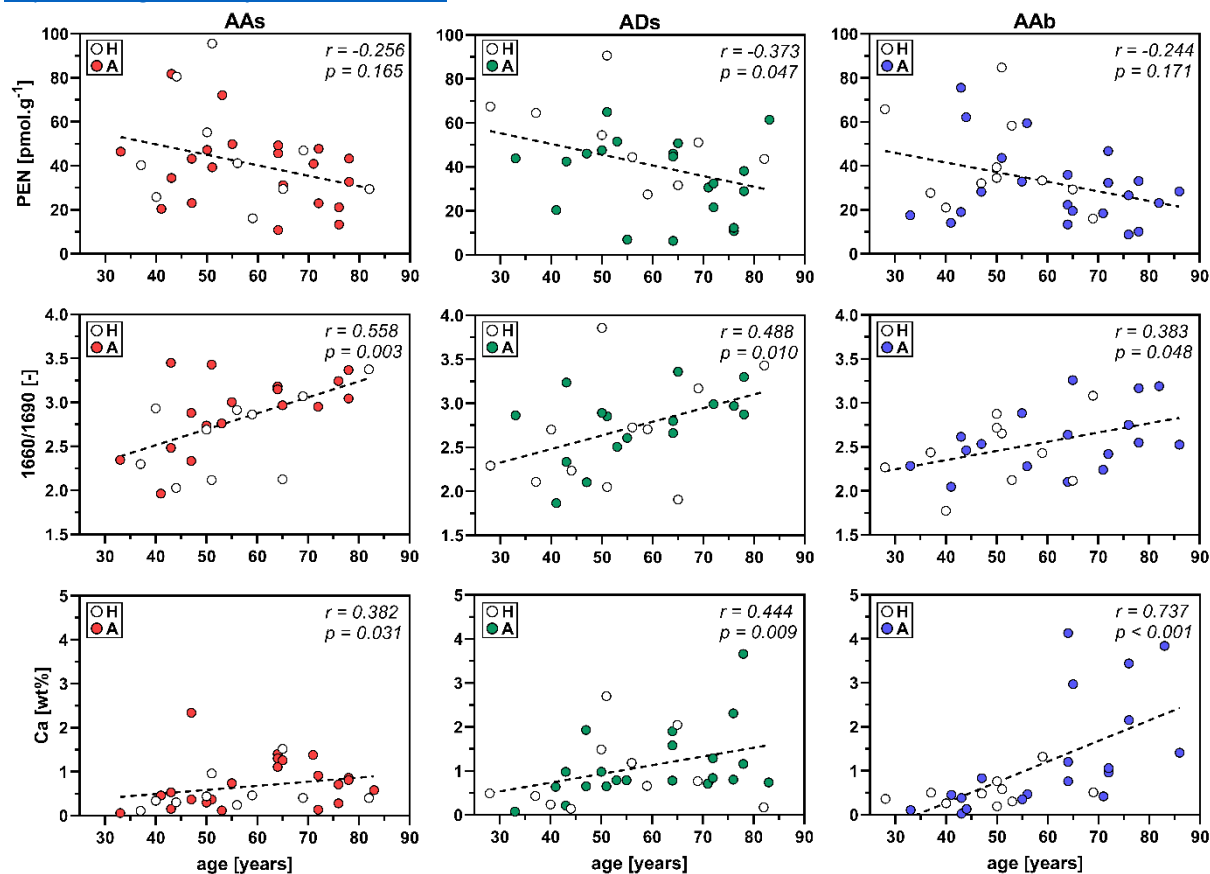


Figure 7. Correlation of PEN, collagen maturation (1660/1690) and the Ca content with the age of the donors for the 3 sections of the aorta. The open circles represent specimens without or with mild signs of atherosclerosis (H), the filled circles represent specimens with atherosclerosis (A). Spearman rank correlation coefficients (r) and two-tailed p -value (p) determined for the pooled data. The linear regression (the dashed line) is shown for illustrative purposes.

3.4 Correlation with the delamination strength

The analysis of the relationship between the chemical and mechanical properties of the arterial wall represented one of the key results of our study. Statistically significant correlations between the biochemical and structural parameters and the delamination strength of the aortic segments aligned in the longitudinal direction of the vessel were observed, particularly with concern to PEN and collagen maturation (Figure 8). The S_d -L correlated positively with the PEN content in all the sections of the aorta ($r = 0.356 - 0.406$, $p < 0.05$). When the data was divided into groups with no or moderate, and with significant atherosclerosis, the correlation was lost for the former group; however, the atherosclerotic aortas continued to exhibit a correlation between PEN and the S_d -L in the AAs segment and, moreover, the correlation was almost significant for the AAb. Regarding the collagen maturation (Figure 8), negative correlations were statistically significant in all the sections of the aorta ($r = -0.567 - -0.422$, $p < 0.05$) except for the AAb, while significant negative correlations were also confirmed for the group of vessels with significant atherosclerosis ($r = -0.688 - -0.488$, $p < 0.05$, all segments). Concerning the other parameters, a particularly negative correlation between the S_d -L and the wall thickness was observed only for the AAb in all the groups, and sporadic correlation was observed between the S_d -L and the intima thickness (pooled data) for the AAs as was the case of the adventitia thickness (positive correlation, AAs, pooled data). No other significant correlations between the S_d -L and the histological parameters were observed. A detailed summary of the Spearman rank correlation coefficients is provided in Table S2 in the Supplement.

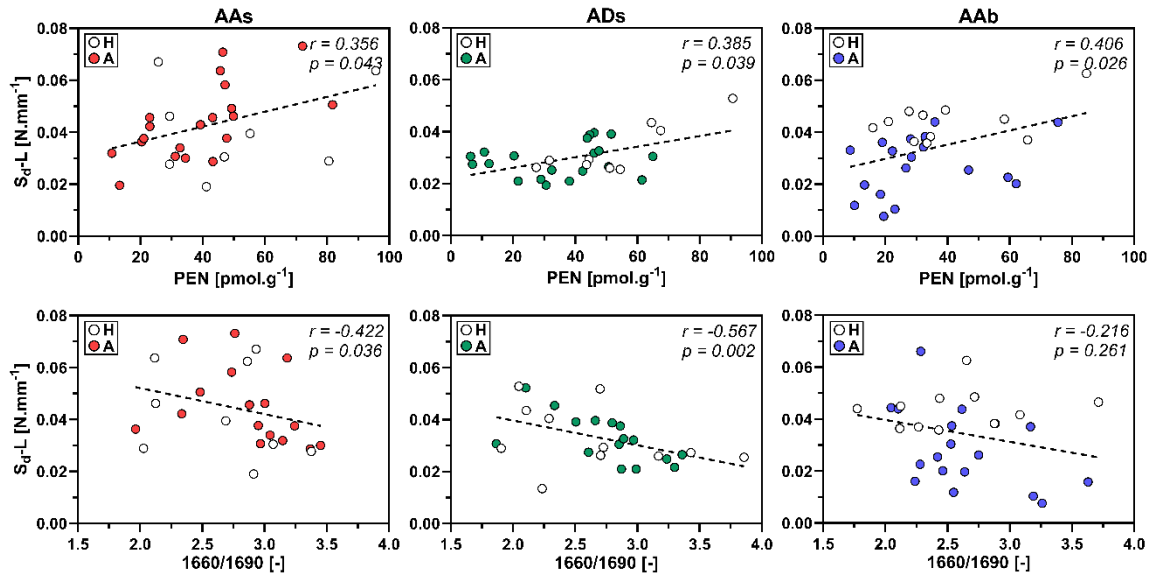


Figure 8. Correlation between PEN and collagen maturation (1660/1690) with the delamination strength in the longitudinal direction (S_{d-L}) in the studied sections of the aorta. The open circles represent specimens without or with mild signs of atherosclerosis (H), the filled circles represent specimens with atherosclerosis (A). Spearman rank correlation coefficients (r) and two-tailed p -value (p) determined for the pooled data. The linear regression (the dashed line) is shown for illustrative purposes.

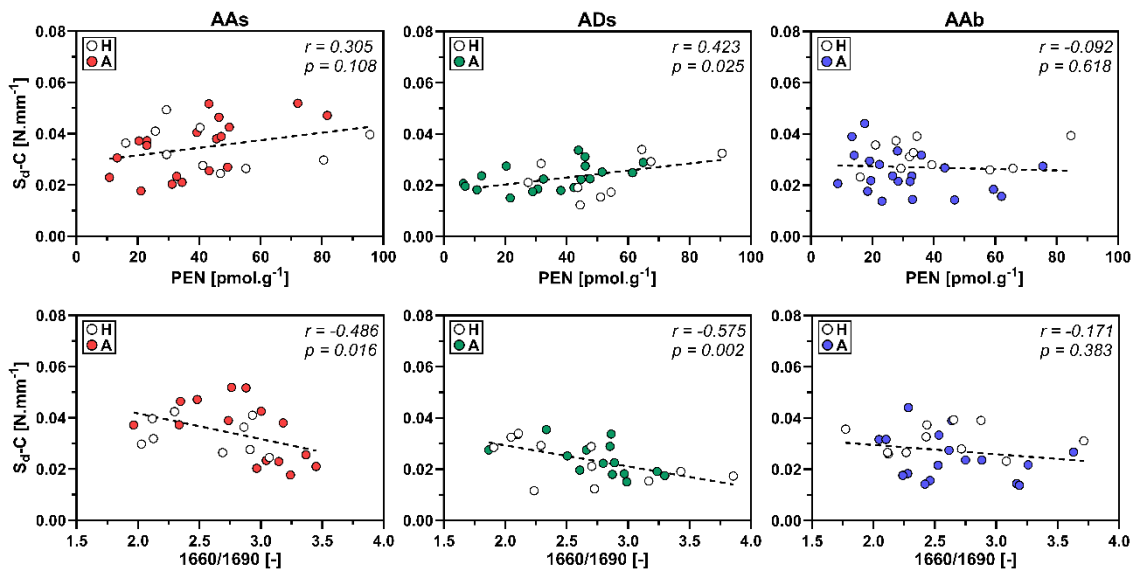


Figure 9. Correlation between PEN and collagen maturation (1660/1690) with the delamination strength in the circumferential direction (S_{d-C}) in the studied sections of the aorta. The open circles represent specimens without or with mild signs of atherosclerosis (H), the filled circles represent specimens with atherosclerosis (A). Spearman rank correlation coefficients (r) and two-tailed p -value (p) determined for the pooled data. The linear regression (the dashed line) is shown for illustrative purposes.

In the case of the S_{d-C} , no statistically significant correlations were observed to the extent detected for the S_{d-L} ; however, an increasing trend was observed for the S_{d-C} with the PEN content, as was a decreasing trend for collagen maturation, which, again, were more pronounced in the merged and atherosclerotic groups (Figure 9). Furthermore, negative correlations were determined for the calcium content in the AAs (pooled data and group A). Concerning the histological parameters, no statistically

significant correlations with the S_{σ} -C were determined, except for the elastin content in the case of the AAs in group A (negative correlation). A detailed summary of the Spearman rank correlation coefficients is provided in Table S3 in the Supplement.

3.5 Effect of the inflammatory environment on the Ca/P ratio

It is known that AGEs contribute to the calcification of the arterial wall [95–97]. The solubility and stability of calcified plaques is influenced by their chemical entity, which can be characterized by the Ca/P ratio. The character of deposits in early and advanced stages of atherosclerosis in human coronary arteries differs significantly in terms of the Ca/P ratio [98]. A high Ca/P ratio of intense calcification may be caused by Ca deposition with another anion, e.g. oxalate, hydroxide or even carbonate, while lower ratios may be due to another inorganic phosphate. As has been proved by several studies [99,100], vascular calcification depends mainly on the balance between the concentration of inorganic phosphate anions and the synthesis of inhibitors, including pyrophosphate (P_2O_7)⁴⁻ anions. In addition, the calcification of atherosclerotic plaques also involves the accumulation of macrophages in the arterial wall. Atherosclerotic lesions contain not only cells that express classical macrophage markers (M1), but also cells that express alternative macrophage markers (M2). M1 macrophages promote inflammation, while M2 macrophages increase pyrophosphate synthesis, which suggests an anti-calcification effect [101]. It is also known that the pH value of advanced atherosclerotic plaques decreases to lower than physiological values (up to 5.5), which, together with the lower pH value caused by the inflammation present in the atherosclerotic tissue, may influence the degree of plaque solubility. Therefore, one of the biochemical parameters investigated in this study concerned the Ca/P weight ratio, which influences the solubility of calcified plaques. The results of the determination of the Ca/P ratio and PEN (Figure 10) revealed an interesting finding on the degree of the stability of calcium phosphate (CaP) plaques in relation to the presence of atherosclerosis. Positive correlation of the Ca/P ratio with the PEN content was detected ($r = 0.410$, $p < 0.05$) in the tissues with no or only mild signs of atherosclerosis, thus indicating an increase in the stability of the CaP deposits. However, concerning the aortic tissues with atherosclerosis, the trend was reversed, i.e. negative correlation with increasing PEN content was observed ($r = -0.356$, $p < 0.05$), thus indicating increasing calcific solubility.

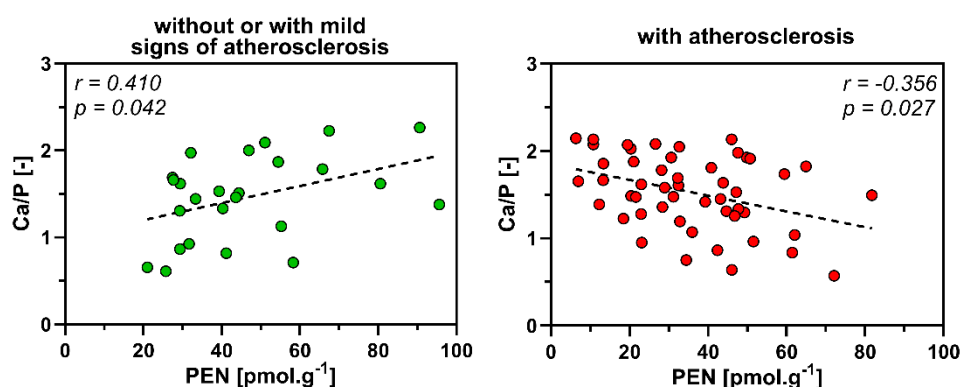


Figure 10. Correlation between the Ca/P ratio and PEN in all the sections of the aorta (pooled data) without or with mild signs of atherosclerosis and with atherosclerosis. Spearman rank correlation coefficients (r), two-tailed p-value (p). The linear regression (the dashed line) is shown for illustrative purposes.

4. Discussion

Aortic dissection is a life-threatening disease that consists of the delamination of the tissue of the aortic wall [2,102–106]. From the mechanical point of view, the formation and propagation of cracks

in dissecting aorta indicates that the mechanical conditions locally exceeded the internal cohesion. The cohesive properties of the arterial wall, which change over the human lifespan due to aging or diseases such as atherosclerosis or arteriosclerosis, are key to understanding aortic dissection [2,16,104–106]. Unfortunately, there remains a lack of data on the biochemical composition of the aortic wall and its relationship to the delamination strength. Thus, the main aim of our study was to provide data on the biochemistry of the human aortic wall and to correlate the data with the delamination strength, and in doing so, to take into account the aging changes to which human tissue is inevitably subjected.

The main result in terms of the delamination properties concerned the statistically significant positive correlation between PEN and the internal cohesion of the aortic wall (Sd-L, Sd-C), Figs. 8 and 9. The correlation was stronger for the longitudinal orientation of the samples which could be associated with the internal organization of the medial layer of the aorta, which contains circumferentially oriented SMC and collagen fibers that, together, create obstacles for tears that propagate in the longitudinal direction. The higher correlation values observed for the longitudinal direction were in agreement with our previous analysis of the correlation between the delamination strength and age [16].

Non-enzymatic crosslinking, attributed to AGEs, has, to date, been investigated from the biomechanical perspective due mainly to its influence on the tensile properties, in connection with which tissue stiffening and changed viscoelasticity have been observed [36,45,46,107–109]. In contrast to the bulk material properties, only a limited number of papers have addressed the relationship between non-enzymatic crosslinking and delamination. Wang et al. [56] performed a study that focused on the effect of glycation on the interlamellar bonding of arterial elastin and found that glucose treatment increased the delamination strength of the aortic walls. Our study suggests a similar conclusion for the entire aortic wall, i.e. both elastin and collagen rather than for the purified elastin network alone or any other individual component.

One of the ways in which AGEs crosslinking may contribute to enhancing the delamination strength is via the reinforcement of radially running collagen fibers, which were proposed as an essential element in terms of the cohesive properties by Pal et al. [110]. Positive correlation between the delamination strength and non-enzymatic glycation expressed via the PEN concentration also appears to be in accordance with clinical findings that suggest that diabetes lowers the risks of dissection and even reduces the mortality rate [57–62].

In contrast to non-enzymatic crosslinking, the maturation of collagen expressed in the FTIR analysis by means of the 1660/1690 sub-band areas revealed negative correlation with the Sd-L and Sd-C (Figures 8 and 9, Tables S2 and S3). The delamination strength decreased significantly with collagen maturation with respect to all the aortic segments in the atherosclerotic aortas group (Sd-L), as well as to the AAs and ADs in the pooled H and A group. Similar results were obtained for the delamination strength as determined for the samples that were delaminated in the circumferential direction (Sd-C). Increasing maturation accompanied by decreasing delamination strength are in agreement with the general concept of age-related changes that act to worsen the physiological conditions of the cardiovascular system.

However, the fact that the results suggest that enzymatic and non-enzymatic crosslinking play contradicting roles in terms of the cohesive properties was somewhat surprising. Enzymatic crosslinking, represented by collagen maturation, correlates negatively with the delamination strength, whereas AGEs-induced non-enzymatic crosslinking led to an increase in this respect. These differing impacts on the material cohesion can theoretically be explained by the different binding sites at which crosslinking occurs. Enzymatic crosslinking is usually described as intra-molecular, whereas non-enzymatic crosslinking has been described as mainly inter-fibrillar [35,37,40]. Collagen that is intra-molecularly reinforced by enzymatic crosslinking may represent an element that more easily

perforates the glycosaminoglycan ground substance of tissues to which it is exposed, while simultaneously evincing enhanced tensile stiffness. Conversely, the inter-fibrillar bonds induced by non-enzymatic crosslinking may exert a limited impact on the tensile properties, but may be engaged in the load carrying process when delamination, considered generally as sliding process, occurs. Nevertheless, at the level of our study, it is not possible to provide a definitive explanation since the spatial arrangement of collagen fibril bundles (intra-laminar fibrils versus radially running inter-laminar fibrils) undoubtedly plays a role in the propagation of tears between the elastic laminae in the tunica media of the aorta.

The results of the determination of age-related changes in the PEN concentration in our study were somewhat surprising. The majority of the papers studied in the literature review indicate that AGEs naturally accumulate in tissues with increasing age [111,112]. However, the results obtained for the available tissues showed that the PEN content rather than increasing with age evinces a decreasing trend, which was statistically insignificant except for the ADs. The occurrence of PEN in tissues may also be affected by a number of metabolic diseases, e.g. diabetes, chronic kidney disease, cardiovascular disease, chronic inflammation associated with autoimmune diseases such as rheumatoid arthritis, etc. [65,113–117]. Although AGEs are elevated primarily in the elderly, they may also be overproduced in younger people under specific conditions such as the enhanced glyco-oxidative loading of the organism, metabolic syndrome or increased oxidative and carbonyl stress. In contrast, a number of studies have shown that the use of certain drugs or antioxidants significantly inhibits the production of AGEs, as well as under certain physiological conditions such as hyperbilirubinemia in Gilbert's syndrome, where bilirubin in the body acts as a very potent antioxidant to prevent the production of AGEs [118]. A further study revealed that the concentrations of AGEs and pentosidine also decrease following a reperfusion injury of the heart (myocardial reperfusion injury) [65]. Therefore, it is possible that our result was influenced by other factors concerning the state of health, which, however, we are unable to comment on since no medical records were available for the purposes of our study. Thus, the reason for the decreasing trend in the PEN content (albeit largely not statistically significant) in the tested aortic tissues remains unknown since the adopted methods, based on the use of cadavers, did not allow us to exclude all the potential sources of uncertainty, especially with regard to details of the health status. Further research employing more detailed clinical data that would allow for the selection of samples according to the diagnosis would contribute significantly to the results of our study; however, this is not possible at the present time.

Interesting data was provided in previous studies that focused on cross-linking and post-translational modifications of the collagen in the dilated and non-dilated aortas of patients with bicuspid aortic valve (BAV) and tricuspid aortic valve (TAV) [119–121]. Wågsäter et al. [119] showed a lower rate of collagen glycation (PEN) in undilated BAV aortas compared to undilated TAV and suggested that BAV is associated with increased collagen turnover in the aorta even prior to the formation of aneurysms. The dilated aortas of TAV patients evinced higher levels of inflammatory markers than those of BAV patients, and the dilated aortas of BAV patients manifested mature collagen fibers and lower collagen turnover, thus suggesting intrinsic aortic fragility. With concern to non-dilated aortas, this study also showed a lower PEN expression in BAV aortas than in TAV aortas, thus suggesting the presence of young collagen and an impaired maturation process. However, it is not possible to generalize based on these observations since patients with BAV, the most common congenital heart disease, represent a mere 1-2% of the population [120,121].

A study by Chung et al. [120] proved that the delamination strength (Sd) of the ascending aorta significantly decreased with age with respect to both outer curvature (OC) and inner curvature (IC) aortic samples, thus demonstrating a strong association between age and Sd. In addition, multivariable linear regression revealed that both the age and BAV were independent predictors of Sd. Moreover, aneurysms in TAV were found to have a lower Sd than those in BAV, even after adjusting for age. They

also proved that BAV is associated with higher degrees of aortic stiffness than is TAV, and that aneurysms in BAV evince a higher delamination strength than in TAV, thus suggesting that the presence of BAV exerts a protective impact.

Age-related changes may also be manifested by other mechanisms that were beyond the scope of this study, e.g. via the content of proteoglycans as the third major component of connective tissues [35]. Such age-related changes at the proteoglycan level may lead to medial degeneration and the development of conditions that facilitate dissection or the formation of aneurysms [103,122]. Cikach et al. [122] focused on proteoglycan accumulation in thoracic aortic aneurysm and dissection (TAAD) and described the molecular changes observed in the aortic wall that promote dilatation and predisposition to dissection such as tissue swelling caused by aggrecan and versican, which is thought to severely impair the mechanics of the aortic wall and smooth muscle cell homeostasis, thus creating a predisposition to dissection. These results suggest that the accumulation of large aggregating proteoglycans may account for the deleterious events in TAAD, and that aggrecan and versican are potential biomarkers of the severity of the disease and the risk of aortic dissection.

It is known that AGEs enhance calcification in vascular tissue [95–97,123]. The results of our study (Fig. 10) confirmed that in this respect one must distinguish between atherosclerosis and arteriosclerosis as different pathological conditions with differing etiologies [28–31]. This is clearly demonstrated in Fig. 10, where the Ca/P ratio highlights the differences in terms of calcification under conditions with and without or with mild signs of atherosclerosis. Indeed, AGEs are essential for the arteriosclerotic (Monckeberg sclerosis) process, which involves predominantly the calcification of the elastic membranes of the tunica media [30,32,124,125]. However, the underlying development of the overall chemical environment of atherosclerotic lesions is altered in the presence of an inflammatory process (inflammation is known to significantly change the pH for example) and we can observe that the effect of PEN was attenuated. Thus, in effect, the atherosclerotic process appears to lead to the formation of calcium phosphate deposits that evince a different solubility than when the influence of age-related AGEs only is involved [126,127].

It should also be noted that our study provides potentially important insights for the mathematical modeling of the cohesive properties of the arterial wall. A large number of mathematical models that describe the mechanics of blood vessels have been reported in the expert literature [8,128,129]. As mechanobiology, which emphasizes the linking of biological processes to the forces carried by cells and tissues, becomes increasingly topical, the need for quantitative biochemical and microstructural data on the vascular wall has increased due to its creating the basis for the structural interpretation of the parameters in mechanobiological constitutive models [5,8,129–132]. In contrast to bulk material properties such as the tensile strength and the elastic modulus, the cohesive properties that are critical for diseases such as aortic dissection have, to date, only rarely been modeled in this way [2,104,105]. One of the reasons concerns the lack of data on the biochemical composition and its relationship to the delamination strength. The correlation of the chemical composition data with the delamination strength provides the basis for the interpretation of the parameters applied in traction-separation laws, which mathematically express the cohesion of the arterial wall [106].

4.1 Limitations of the study

Our study, naturally, has several limitations that should be noted. One of the limitations mentioned previously concerns the fact that since the samples were collected during autopsies, we were unable to access the detailed medical records of the donors. Hence, some of the factors that could theoretically explain, for example, the high variance that did not allow for the drawing of unequivocal conclusions when dividing the donors into the without and with or mild signs of atherosclerosis groups (Fig. 6), remained hidden, which may have confounded the results. Nevertheless, when working with human samples, it is not possible to expect the same conditions as when experimenting with

laboratory animals. Moreover, it should also be taken into account that it is difficult to transfer ageing-induced changes in the human physiology to laboratory models with completely different life expectancies (months versus up to a century). A knowledge of the medical history of the donors would have been advantageous in terms of the interpretation of the findings; however, it is worth noting that our main aim was to determine the causal relationships between the biochemical characteristics obtained and the cohesive properties. Thus, the 3-year collection of tissue represents an essentially random selection process which potentially provides new insights that might not have been detected employing a precisely stratified sample. Thus, our study on the tissue samples obtained primarily reveals those properties that significantly influence the delamination strength.

A further limitation of our study concerned the performance of a wide range of analyses on the same samples. Mechanical tests were performed, the PEN, hydroxyproline and calcium contents were determined, and the FTIR and SEM analyses and the histological evaluations were conducted on each of the sections of the aorta, which placed strict limitations on the weights and the number of samples studied. Whilst the performance of multiple analyses on the same samples was one of the advantages of this study, it inevitably resulted in the restriction of the number of repetitions and, in particular, the low volumes analysed may have led to misleading results or wide variances due to the high degree of heterogeneity of aortic tissue.

The dimensional limitation in terms of obtaining samples led to a certain degree of inaccuracy when assigning the observed values, whether concerning the biomechanical properties or, for example, the biochemical content, to exact positions on the aorta, with regard to both the length-wise direction and the circumference. As detailed in a previous study [16], the delamination strength was in all cases determined for 4 strips with a finite length and width (typically 8 mm x 60 mm). The dimensions of the samples for the biochemical and histological analyses subsequently needed to be added to these dimensions. Thus, the most accurate possible determination of the location at which to assign the detected quantity, e.g. S_d , was 4 x 8 x 60 mm. This did not allow us to specify, for example, how the individual observed quantities were distributed around the circumference of the aorta and should be understood as the average value for the given segment. As discussed in [16], the anatomical segments were sampled in such a way that the proximal part was in all cases the AAs segment and the middle part of the aortic length was always the ADs and AAb segments.

A further limitation associated with the dimensions of the samples concerned the naturally inhomogeneous character of aortic tissue. For example, the determination of the calcium content is fundamentally influenced by the local presence of calcified plaques in the aortic walls. Similarly, the determination of PEN and hydroxyproline is affected by the heterogeneity of the samples, which, moreover, increases with age. The results of the calcium, PEN and hydroxyproline analyses were based on the weight of the vessel portion, which, in addition to the protein portion also contains fat, cholesterol and calcium phosphate (Figures 6, 11 - 13). Thus, the results may have been affected by the biased mass balance; for example, if a substantial part of the sample mass comprises atherosclerotic plaque, the PEN value in the organic part will be higher than in the whole of the sample, the mass of which is substantially affected by the presence of an inorganic component that does not contain PEN. In contrast, the FTIR applied for the evaluation of the ratio 1660/1690 amide I spectral band, i.e. the protein portion, is not impacted by this factor since the spectral bands of cholesterol, lipids and CaP plaques are not present in the amide I band. Therefore heterogeneity does not present a major limitation in terms of the determination of the collagen matrix. The determination of the Ca/P ratio by means of EDS, which was related in this study to the solubility rate of the calcified plaques, was performed from the full wall thickness (further examples of EDS maps are provided in Figures S1 and S2 in the Supplement). Thus, the calcium content, as an element, is influenced by its presence outside calcium deposits, for example, in calcium channels.

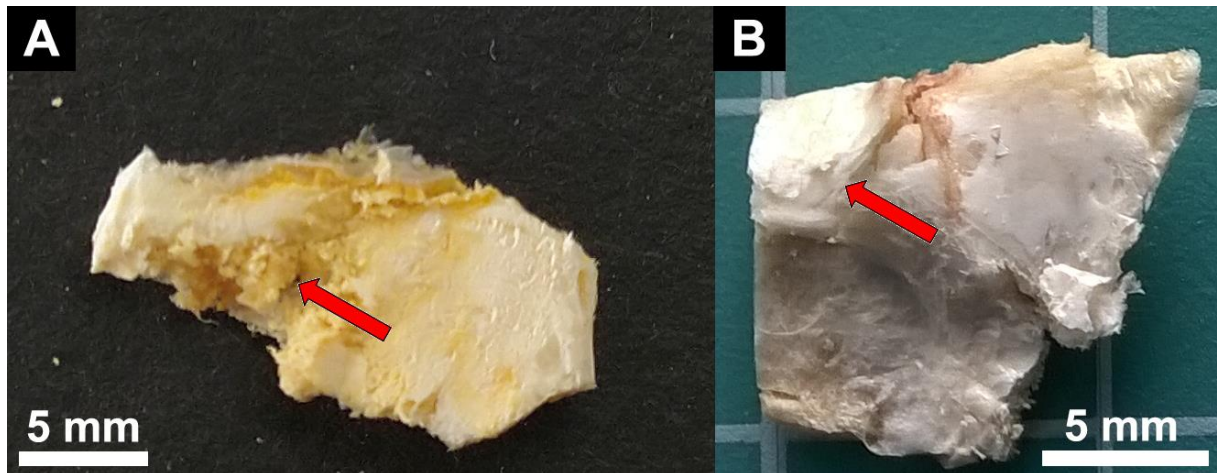


Figure 11. **A:** Example of a break-out section composed of cholesterol, lipids and an apatite mixture in the media part of the AAs (male, 76 years); bar 5 mm. **B:** pathological calcification lesion in the media part of the AAb (male, 64 years); bar 5 mm.

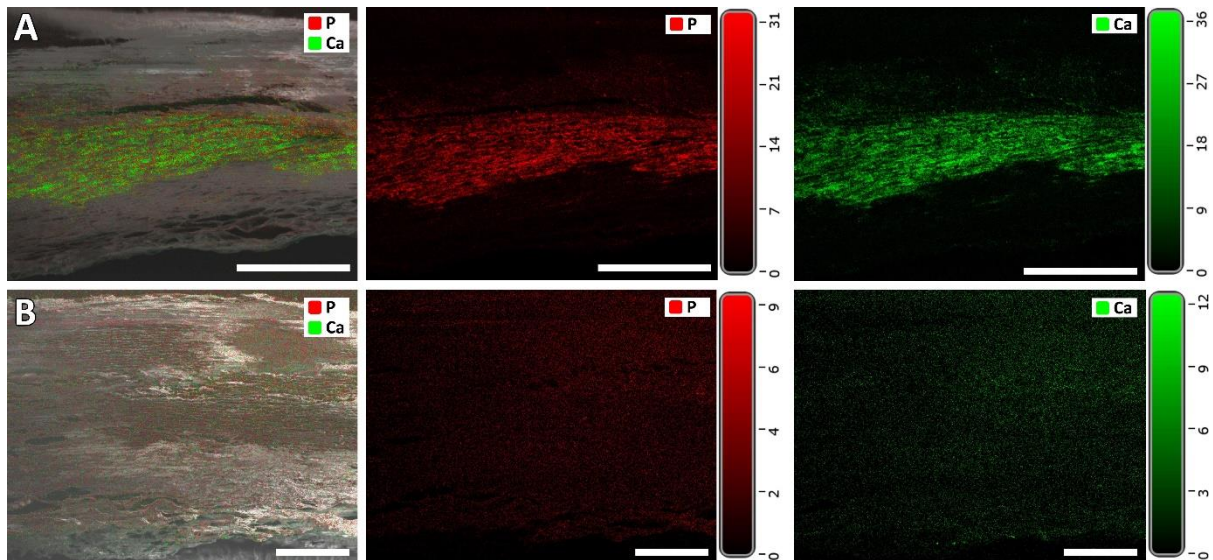


Figure 12. Example of the mapping of calcium and phosphorus elements by means of EDS. **A:** male 65 years, mag. 230x, bar 500 µm; **B:** male 43 years, mag. 150x, bar 500 µm. The color scale represents the weight percentage of the element (Ca or P). The inhomogeneity of the Ca and P distribution is evident from the EDS analysis. The donor B tissue contains a small amount of homogeneously dispersed elements, whereas the donor A tissue probably contains a calcified plaque in the medial part, in the vicinity of which the concentration of both elements is minimal.

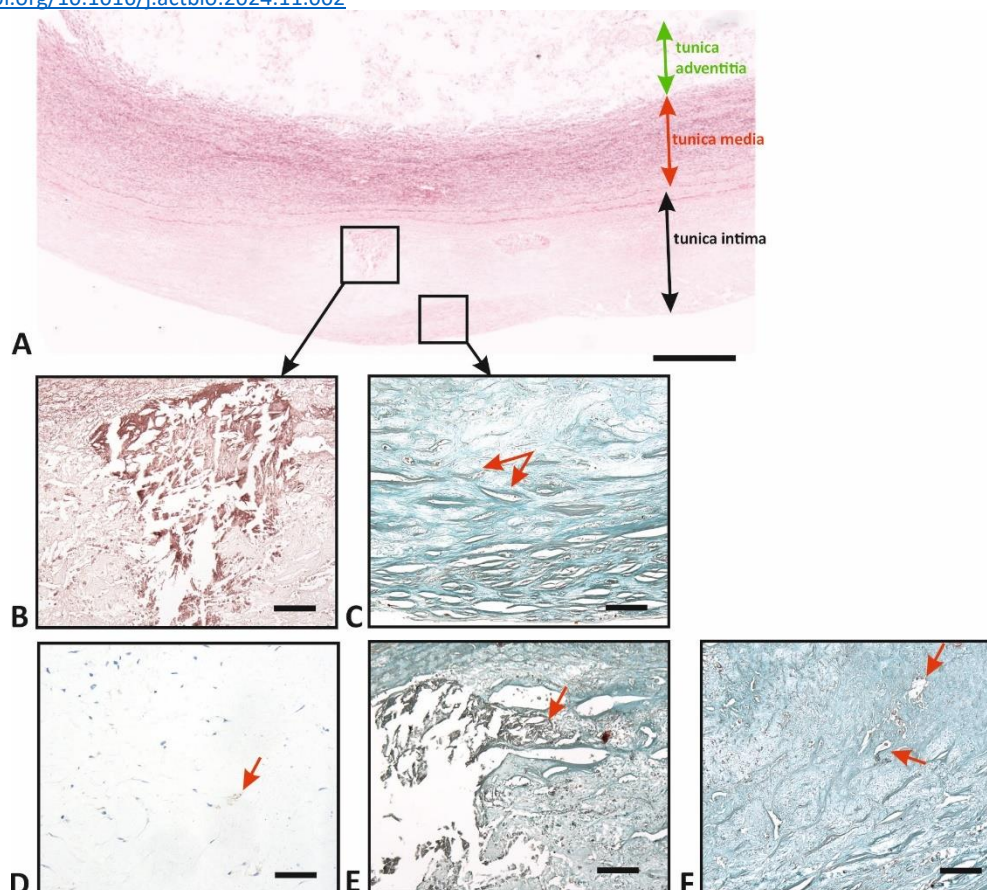


Figure 13. Atherosclerotic lesions. **A** – The abdominal aorta with atherosclerotic changes. Three layers were observed: namely the remodeled tunica intima (progressive intimal fibrosis with accompanying atherosclerotic changes), tunica media, and tunica adventitia. Staining using Orcein. **B** – Atheroma of the aorta, which consists of amorphous material and empty spaces that previously contained lipid-rich material. Staining using Orcein. **C** – Accumulation of lipids (red arrows) in the intima, which are washed out following histological processing, thus leaving empty spaces. Staining using Verhoeff's hematoxylin and green trichrome. **D** – Neovascularization (brown vessels - red arrow) in the intima. Staining using antibody anti-CD31. **E** – Cholesterol crystals (red arrow) in the intima. Staining using Verhoeff's hematoxylin and green trichrome. **F** – Foam cells (macrophages phagocytize lipid and transformation into foam cells - red arrows) in the intima of the aorta wall. Staining using Verhoeff's hematoxylin and green trichrome. Scale bars 500 μm (A) and 50 μm (B-F).

5. Conclusion

This study addressed the correlation of the delamination strength with the results of the comprehensive biochemical and histological analysis of the human aortic wall collected via the examination of 34 cadavers during regular autopsies. The study further aimed to correlate the changes in the composition with age. A total of 16 parameters were determined and correlation was sought with the delamination forces in both the longitudinal and circumferential directions of the vessel as determined using identical samples. The measured parameters comprised the pentosidine, hydroxyproline and calcium contents, the calcium/phosphorus molar ratio, the degree of atherosclerosis, the area fraction of elastin, collagen type I and III, alpha smooth muscle actin, vasa vasorum, the vasa vasorum density, the aortic wall thickness, and the thicknesses of the adventitia, media and intima determined by means of quantitative histology.

The results show that the vast majority of the quantities determined did not correlate with age, with the exception of the calcium content and collagen maturation (enzymatic crosslinking). A further interesting finding concerned the decreasing trend of the pentosidine content with age (in most cases without statistical significance), which was most likely due to the differing medical histories of the donors, a factor that could not be determined.

The main results refer to the differences between the enzymatic and non-enzymatic crosslinking and the differences caused by the presence of atherosclerosis. It was shown that whereas the non-enzymatic crosslinking of collagen tends to decrease with age, and in doing so increases with the delamination strength, the enzymatic crosslinking of collagen evinces the opposite trend, i.e. the rate of maturation increases with age accompanied by a decrease in the delamination strength of the wall. The results suggest that enzymatic and non-enzymatic crosslinking play contradicting roles in terms of the cohesive properties. These opposing effects may well be related to the different binding sites at which collagen and elastin enzymatic and non-enzymatic crosslinking occur in their complex hierarchical structure. Although our results were burdened by a degree of variability that, in some cases, prevented the determination of the statistical significance of the observed differences, the positive correlation between the pentosidine content and the delamination strength is particularly consistent with knowledge on the course of aortic dissection in diabetic patients obtained from the clinical setting.

The results also revealed an interesting trend in terms of the molar ratio of calcium and phosphorus, which reflected the differing solubility rates of the calcium phosphate plaques present in the aortic tissue samples analyzed. Assuming that AGEs (PEN) contribute to the calcification of the arterial wall, it was observed that the Ca/P ratio increases with increasing degrees of calcification in tissues without or with mild signs of atherosclerosis. Concerning tissues affected by atherosclerosis, this ratio decreases with the increasing rate of calcification. This may indicate that as the rate of calcification increases, the presence of atherosclerosis leads to the formation of calcium phosphate plaques with a higher solubility than in the case of tissue without or with mild signs of atherosclerosis. This process may be associated with inflammation and a decrease in the pH in the presence of atherosclerosis.

The contribution of this study lies in the detailed biochemical comparison of the enzymatic and non-enzymatic crosslinks of vascular tissues and their influence on the delamination parameters since, to the best of our knowledge, no such comprehensive studies exist in the literature. A further benefit concerns the notification of the limitations of the various analytical methods applied, which is an important factor that must be taken into account in such studies. We believe that our study also provides potentially important insights for the mathematical modeling of the cohesive properties of the arterial wall by providing the basis for the interpretation of the parameters applied via traction-separation laws.

Acknowledgments

This study was supported by the Czech Science Foundation under project no. GA20-11186S entitled “Mechanics of Arterial Delamination and Crack Propagation”. The study (histological evaluation) received support from the Charles University Cooperatio Programme, research area MED/DIAG. O.Y was supported by EMBO, grant no. SLG 5433. We gratefully acknowledge the financial support provided for our work by the Long-term Conceptual Development Research Organization under project no. RVO: 67985891. Special thanks go to Mr. Darren Ireland (BA (Hons), Cert. ed.) for the language revision of the English manuscript.

References

- [1] G.S. Kassab, Biomechanics of the cardiovascular system: the aorta as an illustratory example, *J. R. Soc. Interface.* 3 (2006) 719–740. <https://doi.org/10.1098/rsif.2006.0138>.
- [2] S. Sherifova, G.A. Holzapfel, Biomechanics of aortic wall failure with a focus on dissection and aneurysm: A review, *Acta Biomater.* 99 (2019) 1–17. <https://doi.org/10.1016/j.actbio.2019.08.017>.
- [3] R. Wang, J.M. Mattson, Y. Zhang, Effect of aging on the biaxial mechanical behavior of human descending thoracic aorta: Experiments and constitutive modeling considering collagen crosslinking., *J. Mech. Behav. Biomed. Mater.* 140 (2023) 105705. <https://doi.org/10.1016/j.jmbbm.2023.105705>.
- [4] T.C. Gasser, *Vascular Biomechanics*, Springer International Publishing, Cham, 2021. <https://doi.org/10.1007/978-3-030-70966-2>.
- [5] T.C. Gasser, R.W. Ogden, G.A. Holzapfel, Hyperelastic modelling of arterial layers with distributed collagen fibre orientations, *J. R. Soc. Interface.* 3 (2005) 15–35. <https://doi.org/10.1098/rsif.2005.0073>.
- [6] J.M. Clark, S. Glagov, Transmural organization of the arterial media. The lamellar unit revisited., *Arteriosclerosis.* 5 (1985) 19–34. <https://doi.org/10.1161/01.atv.5.1.19>.
- [7] M. O’Connell, S. Murthy, S. Phan, C. Xu, J. Buchanan, R. Spilker, R. Dalman, C. Zarins, W. Denk, C. Taylor, The three-dimensional micro- and nanostructure of the aortic medial lamellar unit measured using 3D confocal and electron microscopy imaging☆, *Matrix Biol.* 27 (2008) 171–181. <https://doi.org/10.1016/j.matbio.2007.10.008>.
- [8] G.A. Holzapfel, T.C. Gasser, R.W. Ogden, A New Constitutive Framework for Arterial Wall Mechanics and a Comparative Study of Material Models, *J. Elast. Phys. Sci. Solids.* 61 (2000) 1–48. <https://doi.org/10.1023/A:1010835316564>.
- [9] Z. Tonar, P. Tomášek, P. Loskot, J. Janáček, M. Králíčková, K. Witter, Vasa vasorum in the tunica media and tunica adventitia of the porcine aorta, *Ann. Anat. - Anat. Anzeiger.* 205 (2016) 22–36. <https://doi.org/10.1016/j.aanat.2016.01.008>.
- [10] M. Grajciarová, D. Turek, A. Malečková, R. Pálek, V. Liška, P. Tomášek, M. Králíčková, Z. Tonar, Are ovine and porcine carotid arteries equivalent animal models for experimental cardiac surgery: A quantitative histological comparison, *Ann. Anat. - Anat. Anzeiger.* 242 (2022) 151910. <https://doi.org/https://doi.org/10.1016/j.aanat.2022.151910>.
- [11] K. Witter, Z. Tonar, H. Schöpfer, How many Layers has the Adventitia? – Structure of the Arterial Tunica Externa Revisited, *Anat. Histol. Embryol.* 46 (2017) 110–120. <https://doi.org/10.1111/ah.12239>.
- [12] T. Voňavková, L. Horný, Effect of axial prestretch and adipose tissue on the inflation-extension behavior of the human abdominal aorta., *Comput. Methods Biomech. Biomed. Engin.* 23 (2020) 81–91. <https://doi.org/10.1080/10255842.2019.1699544>.
- [13] L. Horný, T. Adamek, M. Kulvajtova, Analysis of axial prestretch in the abdominal aorta with reference to post mortem interval and degree of atherosclerosis, *J. Mech. Behav. Biomed. Mater.* 33 (2014) 93–98. <https://doi.org/https://doi.org/10.1016/j.jmbbm.2013.01.033>.
- [14] S. Roccabianca, C.A. Figueroa, G. Tellides, J.D. Humphrey, Quantification of regional differences in aortic stiffness in the aging human, *J. Mech. Behav. Biomed. Mater.* 29 (2014) 618–634. <https://doi.org/10.1016/j.jmbbm.2013.01.026>.
- [15] L. Horný, M. Netušil, M. Daniel, Limiting extensibility constitutive model with distributed fibre orientations and ageing of abdominal aorta, *J. Mech. Behav. Biomed. Mater.* 38 (2014) 39–51. <https://doi.org/https://doi.org/10.1016/j.jmbbm.2014.05.021>.
- [16] L. Horný, L. Roubalová, J. Kronek, H. Chlup, T. Adámek, A. Blanková, Z. Petřivý, T. Suchý, P. Tichý, Correlation between age, location, orientation, loading velocity and delamination strength in the human aorta, *J. Mech. Behav. Biomed. Mater.* 133 (2022) 105340. <https://doi.org/https://doi.org/10.1016/j.jmbbm.2022.105340>.
- [17] J.A. Niestrawska, C. Viertler, P. Regitnig, T.U. Cohnert, G. Sommer, G.A. Holzapfel, Microstructure and mechanics of healthy and aneurysmatic abdominal aortas: experimental analysis and modelling, *J. R. Soc. Interface.* 13 (2016) 20160620. <https://doi.org/10.1098/rsif.2016.0620>.
- [18] F.L. Wuyts, V.J. Vanhuysse, G.J. Langewouters, W.F. Decraemer, E.R. Raman, S. Buyle, Elastic properties of human aortas in relation to age and atherosclerosis: a structural model, *Phys. Med. Biol.* 40 (1995) 1577–1597. <https://doi.org/10.1088/0031-9155/40/10/002>.
- [19] M. Amabili, P. Balasubramanian, I. Bozzo, I.D. Breslavsky, G. Ferrari, Layer-specific hyperelastic and viscoelastic characterization of human descending thoracic aortas, *J. Mech. Behav. Biomed. Mater.* 99 (2019) 27–46. <https://doi.org/https://doi.org/10.1016/j.jmbbm.2019.07.008>.
- [20] M. Jadidi, W. Poulson, P. Aylward, J. MacTaggart, C. Sanderfer, B. Marmie, M. Pipinos, A. Kamenskiy,

- Calcification prevalence in different vascular zones and its association with demographics, risk factors, and morphometry, *Am. J. Physiol. Circ. Physiol.* 320 (2021) H2313–H2323. <https://doi.org/10.1152/ajpheart.00040.2021>.
- [21] M. Jadidi, S.A. Razian, M. Habibnezhad, E. Anttila, A. Kamenskiy, Mechanical, structural, and physiologic differences in human elastic and muscular arteries of different ages: Comparison of the descending thoracic aorta to the superficial femoral artery, *Acta Biomater.* 119 (2021) 268–283. <https://doi.org/https://doi.org/10.1016/j.actbio.2020.10.035>.
- [22] H. Weisbecker, D.M. Pierce, P. Regitnig, G.A. Holzapfel, Layer-specific damage experiments and modeling of human thoracic and abdominal aortas with non-atherosclerotic intimal thickening, *J. Mech. Behav. Biomed. Mater.* 12 (2012) 93–106. <https://doi.org/10.1016/j.jmbbm.2012.03.012>.
- [23] A. V Kamenskiy, Y.A. Dzenis, S.A.J. Kazmi, M.A. Pemberton, I.I. Pipinos, N.Y. Phillips, K. Herber, T. Woodford, R.E. Bowen, C.S. Lomneth, J.N. MacTaggart, Biaxial mechanical properties of the human thoracic and abdominal aorta, common carotid, subclavian, renal and common iliac arteries, *Biomech. Model. Mechanobiol.* 13 (2014) 1341–1359. <https://doi.org/10.1007/s10237-014-0576-6>.
- [24] M.R. Labrosse, E.R. Gerson, J.P. Veinot, C.J. Beller, Mechanical characterization of human aortas from pressurization testing and a paradigm shift for circumferential residual stress, *J. Mech. Behav. Biomed. Mater.* 17 (2013) 44–55. <https://doi.org/https://doi.org/10.1016/j.jmbbm.2012.08.004>.
- [25] G.A. Holzapfel, G. Sommer, C.T. Gasser, P. Regitnig, Determination of layer-specific mechanical properties of human coronary arteries with nonatherosclerotic intimal thickening and related constitutive modeling, *Am. J. Physiol. Circ. Physiol.* 289 (2005) H2048–H2058. <https://doi.org/10.1152/ajpheart.00934.2004>.
- [26] E.G. Lakatta, The reality of aging viewed from the arterial wall ☆, *Artery Res.* 7 (2013) 73. <https://doi.org/10.1016/j.artres.2013.01.003>.
- [27] J.M. Phillip, I. Aifuwa, J. Walston, D. Wirtz, The Mechanobiology of Aging, *Annu. Rev. Biomed. Eng.* 17 (2015) 113–141. <https://doi.org/10.1146/annurev-bioeng-071114-040829>.
- [28] S.E. Greenwald, Ageing of the conduit arteries, *J. Pathol.* 211 (2007) 157–172. <https://doi.org/https://doi.org/10.1002/path.2101>.
- [29] M.F. O'Rourke, J. Hashimoto, Mechanical Factors in Arterial Aging, *J. Am. Coll. Cardiol.* 50 (2007) 1–13. <https://doi.org/10.1016/j.jacc.2006.12.050>.
- [30] V. Persy, P. D'Haese, Vascular calcification and bone disease: the calcification paradox, *Trends Mol. Med.* 15 (2009) 405–416. <https://doi.org/10.1016/j.molmed.2009.07.001>.
- [31] B.R. Kwak, M. Bäck, M.-L. Bochaton-Piallat, G. Caligiuri, M.J.A.P. Daemen, P.F. Davies, I.E. Hofer, P. Holvoet, H. Jo, R. Krams, S. Lehoux, C. Monaco, S. Steffens, R. Virmani, C. Weber, J.J. Wentzel, P.C. Evans, Biomechanical factors in atherosclerosis: mechanisms and clinical implications, *Eur. Heart J.* 35 (2014) 3013–3020. <https://doi.org/10.1093/eurheartj/ehu353>.
- [32] R.W. Jayalath, S.H. Mangan, J. Golledge, Aortic Calcification, *Eur. J. Vasc. Endovasc. Surg.* 30 (2005) 476–488. <https://doi.org/https://doi.org/10.1016/j.ejvs.2005.04.030>.
- [33] L. Horný, *Cardiovascular Mechanics*, CRC Press, Boca Raton, FL : CRC Press/Taylor & Francis Group, [2018], 2018. <https://doi.org/10.1201/b21917>.
- [34] C.M. McEniery, B.J. McDonnell, A. So, S. Aitken, C.E. Bolton, M. Munnery, S.S. Hickson, null Yasmin, K.M. Maki-Petaja, J.R. Cockcroft, A.K. Dixon, I.B. Wilkinson, Aortic Calcification Is Associated With Aortic Stiffness and Isolated Systolic Hypertension in Healthy Individuals, *Hypertension.* 53 (2009) 524–531. <https://doi.org/10.1161/HYPERTENSIONAHA.108.126615>.
- [35] A.J. Bailey, Molecular mechanisms of ageing in connective tissues., *Mech. Ageing Dev.* 122 (2001) 735–755. [https://doi.org/10.1016/s0047-6374\(01\)00225-1](https://doi.org/10.1016/s0047-6374(01)00225-1).
- [36] E. Konova, S. Baydanoff, M. Atanasova, A. Velkova, Age-related changes in the glycation of human aortic elastin, *Exp. Gerontol.* 39 (2004) 249–254. <https://doi.org/https://doi.org/10.1016/j.exger.2003.10.003>.
- [37] N.C. Avery, A.J. Bailey, Restraining Cross-Links Responsible for the Mechanical Properties of Collagen Fibers: Natural and Artificial BT - Collagen: Structure and Mechanics, in: P. Fratzl (Ed.), Springer US, Boston, MA, 2008: pp. 81–110. https://doi.org/10.1007/978-0-387-73906-9_4.
- [38] M.J. Sherratt, Tissue elasticity and the ageing elastic fibre, *Age (Omaha).* 31 (2009) 305–325. <https://doi.org/10.1007/s11357-009-9103-6>.
- [39] S.P. Robins, Biochemistry and functional significance of collagen cross-linking, *Biochem. Soc. Trans.* 35 (2007) 849–852. <https://doi.org/10.1042/BST0350849>.
- [40] L. Knott, A.J. Bailey, Collagen cross-links in mineralizing tissues: A review of their chemistry, function, and clinical relevance, *Bone.* 22 (1998) 181–187. <https://doi.org/https://doi.org/10.1016/S8756->

- 3282(97)00279-2.
- [41] W.-H. Hui, Y.-L. Chen, S.-W. Chang, Effects of aging and diabetes on the deformation mechanisms and molecular structural characteristics of collagen fibrils under daily activity, *Int. J. Biol. Macromol.* 254 (2024) 127603. <https://doi.org/10.1016/j.ijbiomac.2023.127603>.
- [42] G. Wolf, K. Sharma, F.N. Ziyadeh, CHAPTER 78 - Pathophysiology and Pathogenesis of Diabetic Nephropathy, in: R.J. ALPERN, S.C.B.T.-S. and G.T.K. (Fourth E. HEBERT (Eds.), Academic Press, San Diego, 2008: pp. 2215–2233. <https://doi.org/https://doi.org/10.1016/B978-012088488-9.50081-4>.
- [43] T.B. McKay, S. Priyadarsini, D. Karamichos, Mechanisms of collagen crosslinking in diabetes and keratoconus, *Cells.* 8 (2019) 1–28. <https://doi.org/10.3390/cells8101239>.
- [44] C. Brasselet, E. Durand, F. Addad, A.A.H. Zen, M.B. Smeets, D. Laurent-Maquin, S. Bouthors, G. Bellon, D. de Kleijn, G. Godeau, R. Garnotel, B. Gogly, A. Lafont, Collagen and elastin cross-linking: a mechanism of constrictive remodeling after arterial injury, *Am. J. Physiol. Circ. Physiol.* 289 (2005) H2228–H2233. <https://doi.org/10.1152/ajpheart.00410.2005>.
- [45] T.J. Sims, L.M. Rasmussen, H. Oxlund, A.J. Bailey, The role of glycation cross-links in diabetic vascular stiffening, *Diabetologia.* 39 (1996) 946–951. <https://doi.org/10.1007/BF00403914>.
- [46] C.P. Winlove, K.H. Parker, N.C. Avery, A.J. Bailey, Interactions of elastin and aorta with sugars in vitro and their effects on biochemical and physical properties, *Diabetologia.* 39 (1996) 1131–1139. <https://doi.org/10.1007/BF02658498>.
- [47] D. De, N. Pawar, A.N. Gupta, Glucose-induced structural changes and anomalous diffusion of elastin, *Colloids Surfaces B Biointerfaces.* 188 (2020) 110776. <https://doi.org/https://doi.org/10.1016/j.colsurfb.2020.110776>.
- [48] D.R. Sell, R.H. Nagaraj, S.K. Grandhee, P. Odetti, A. Lapolla, J. Fogarty, V.M. Monnier, Pentosidine: A molecular marker for the cumulative damage to proteins in diabetes, aging, and uremia, *Diabetes. Metab. Rev.* 7 (1991) 239–251. <https://doi.org/10.1002/dmr.5610070404>.
- [49] V.M. Monnier, N. Taniguchi, Advanced glycation in diabetes, aging and age-related diseases: conclusions, *Glycoconj. J.* 33 (2016) 691–692. <https://doi.org/10.1007/s10719-016-9711-1>.
- [50] M. Braun, Pentosidine, an Advanced Glycation End-Product, May Reflect Clinical and Morphological Features of Hand Osteoarthritis, *Open Rheumatol. J.* 6 (2012) 64–69. <https://doi.org/10.2174/1874312901206010064>.
- [51] M. Kalousová, T. Zima, V. Tesař, S. Štípek, S. Sulková, Advanced Glycation End Products in Clinical Nephrology, *Kidney Blood Press. Res.* 27 (2004) 18–28. <https://doi.org/10.1159/000075533>.
- [52] K. Taki, F. Takayama, Y. Tsuruta, T. Niwa, Oxidative stress, advanced glycation end product, and coronary artery calcification in hemodialysis patients, *Kidney Int.* 70 (2006) 218–224. <https://doi.org/10.1038/sj.ki.5000330>.
- [53] M.A. Lillie, J.M. Gosline, Swelling and viscoelastic properties of osmotically stressed elastin., *Biopolymers.* 39 (1996) 641–652. [https://doi.org/10.1002/\(sici\)1097-0282\(199611\)39:5<641::aid-bip3>3.0.co;2-w](https://doi.org/10.1002/(sici)1097-0282(199611)39:5<641::aid-bip3>3.0.co;2-w).
- [54] Y. Zou, Y. Zhang, The Biomechanical Function of Arterial Elastin in Solute, *J. Biomech. Eng.* 134 (2012). <https://doi.org/10.1115/1.4006593>.
- [55] Y. Wang, S. Zeinali-Davarani, E.C. Davis, Y. Zhang, Effect of glucose on the biomechanical function of arterial elastin, *J. Mech. Behav. Biomed. Mater.* 49 (2015) 244–254. <https://doi.org/10.1016/j.jmbbm.2015.04.025>.
- [56] R. Wang, X. Yu, A. Gkousioudi, Y. Zhang, Effect of Glycation on Interlamellar Bonding of Arterial Elastin, *Exp. Mech.* 61 (2021) 81–94. <https://doi.org/10.1007/s11340-020-00644-y>.
- [57] S.K. Prakash, C. Pedroza, Y.A. Khalil, D.M. Milewicz, Diabetes and Reduced Risk for Thoracic Aortic Aneurysms and Dissections: A Nationwide Case-Control Study, *J. Am. Heart Assoc.* 1 (2012). <https://doi.org/10.1161/JAHA.111.000323>.
- [58] N.S. Theivacumar, M.A. Stephenson, H. Mistry, D. Valenti, Diabetics Are Less Likely to Develop Thoracic Aortic Dissection: A 10-Year Single-Center Analysis, *Ann. Vasc. Surg.* 28 (2014) 427–432. <https://doi.org/10.1016/j.avsg.2013.03.024>.
- [59] I. Jiménez-Trujillo, M. González-Pascual, R. Jiménez-García, V. Hernández-Barrera, J.M. de Miguel-Yanes, M. Méndez-Bailón, J. de Miguel-Diez, M.Á. Salinero-Fort, N. Perez-Farinos, P. Carrasco-Garrido, A. López-de-Andrés, Type 2 Diabetes Mellitus and Thoracic Aortic Aneurysm and Dissection: An Observational Population-Based Study in Spain From 2001 to 2012, *Medicine (Baltimore).* 95 (2016).
- [60] H. Takagi, T. Umemoto, Negative Association of Diabetes With Thoracic Aortic Dissection and Aneurysm, *Angiology.* 68 (2017) 216–224. <https://doi.org/10.1177/0003319716647626>.
- [61] T. Avdic, S. Franzén, M. Zarrouk, S. Acosta, P. Nilsson, A. Gottsäter, A. Svensson, S. Gudbjörnsdóttir, B.

- Eliasson, Reduced Long-Term Risk of Aortic Aneurysm and Aortic Dissection Among Individuals With Type 2 Diabetes Mellitus: A Nationwide Observational Study, *J. Am. Heart Assoc.* 7 (2024) e007618. <https://doi.org/10.1161/JAHA.117.007618>.
- [62] H. Liu, L. Shi, T. Zeng, Q. Ji, Y. Shi, Y. Huang, L. Zhang, T. Xiao, J. Ye, Y. Lin, L. Liu, Type 2 diabetes mellitus reduces clinical complications and mortality in Stanford type B aortic dissection after thoracic endovascular aortic repair: A 3-year follow-up study, *Life Sci.* 230 (2019) 104–110. <https://doi.org/10.1016/j.lfs.2019.05.055>.
- [63] R. Shahbad, A. Kamenskiy, S.A. Razian, M. Jadidi, A. Desyatova, Effects of Age, Elastin Density, and Glycosaminoglycan Accumulation on the Delamination Strength of Human Thoracic and Abdominal Aortas, *Acta Biomater.* (2024). <https://doi.org/10.1016/j.actbio.2024.10.010>.
- [64] V. Kumar, others, Robbins and Cotran pathologic basis of disease, in: Robbins Cotran Pathol. Basis Dis., 2010: pp. xiv--1450.
- [65] P. Celec, J. Hodosy, P. Jáni, P. Janega, M. Kúdela, M. Kalousová, J. Holzerová, V. Parrák, L. Halčák, T. Zima, M. Braun, I. Pecháň, J. Murín, K. Šebeková, Advanced glycation end products in myocardial reperfusion injury, *Heart Vessels.* 27 (2012) 208–215. <https://doi.org/10.1007/s00380-011-0147-z>.
- [66] K. Yanagisawa, Z. Makita, K. Shiroshita, T. Ueda, T. Fusegawa, S. Kuwajima, M. Takeuchi, T. Koike, Specific fluorescence assay for advanced glycation end products in blood and urine of diabetic patients, *Metabolism.* 47 (1998) 1348–1353. [https://doi.org/10.1016/S0026-0495\(98\)90303-1](https://doi.org/10.1016/S0026-0495(98)90303-1).
- [67] M. Pia de la Maza, F. Garrido, N. Escalante, L. Leiva, G. Barrera, S. Schnitzler, M. Zanolli, J. Verdaguer, S. Hirsch, N. Jara, D. Bunout, Fluorescent advanced glycation end-products (ages) detected by spectro-photofluorimetry, as a screening tool to detect diabetic microvascular complications, *J. Diabetes Mellit.* 02 (2012) 221–226. <https://doi.org/10.4236/jdm.2012.22035>.
- [68] C. Sady, S. Khosrof, R. Nagaraj, Advanced Maillard Reaction and Crosslinking of Corneal Collagen in Diabetes, *Biochem. Biophys. Res. Commun.* 214 (1995) 793–797. <https://doi.org/10.1006/bbrc.1995.2356>.
- [69] P. Špaček, M. Adam, Pentosidine in osteoarthritis: HPLC determination in body fluids and in tissues, *Rheumatol. Int.* 26 (2006) 923–927. <https://doi.org/10.1007/s00296-006-0105-8>.
- [70] A. Singla, C.H. Lee, Effect of elastin on the calcification rate of collagen-elastin matrix systems, *J. Biomed. Mater. Res.* 60 (2002) 368–374. <https://doi.org/10.1002/jbm.10077>.
- [71] R. Cheheltani, C.M. McGovern, J. Rao, D.A. Vorp, M.F. Kiani, N. Pleshko, Fourier transform infrared spectroscopy to quantify collagen and elastin in an in vitro model of extracellular matrix degradation in aorta, *Analyst.* 139 (2014) 3039–3047. <https://doi.org/10.1039/C3AN02371K>.
- [72] R. Cheheltani, J.E. Pichamuthu, J. Rao, J.S. Weinbaum, M.F. Kiani, D.A. Vorp, N. Pleshko, Fourier Transform Infrared Spectroscopic Imaging-Derived Collagen Content and Maturity Correlates with Stress in the Aortic Wall of Abdominal Aortic Aneurysm Patients, *Cardiovasc. Eng. Technol.* 8 (2017) 70–80. <https://doi.org/10.1007/s13239-016-0289-3>.
- [73] M. Houška, A. Landfeld, P. Novotná, J. Strohalm, M. Šupová, T. Suchý, H. Chlup, J. Skočilas, J. Štípek, M. Žaloudková, M. Šulc, Properties of Bovine Collagen as Influenced by High-Pressure Processing, *Polymers (Basel).* 15 (2023). <https://doi.org/10.3390/polym15112472>.
- [74] K.J. Payne, A. Veis, Fourier transform ir spectroscopy of collagen and gelatin solutions: Deconvolution of the amide I band for conformational studies, *Biopolymers.* 27 (1988) 1749–1760. <https://doi.org/10.1002/bip.360271105>.
- [75] D.A. Prystupa, A.M. Donald, Infrared study of gelatin conformations in the gel and sol states, *Polym. Gels Networks.* 4 (1996) 87–110. [https://doi.org/10.1016/0966-7822\(96\)00003-2](https://doi.org/10.1016/0966-7822(96)00003-2).
- [76] M. Jackson, L.P. Choo, P.H. Watson, W.C. Halliday, H.H. Mantsch, Beware of connective tissue proteins: assignment and implications of collagen absorptions in infrared spectra of human tissues., *Biochim. Biophys. Acta.* 1270 (1995) 1–6. [https://doi.org/10.1016/0925-4439\(94\)00056-v](https://doi.org/10.1016/0925-4439(94)00056-v).
- [77] A. Pielesz, Temperature-dependent FTIR spectra of collagen and protective effect of partially hydrolysed fucoidan, *Spectrochim. Acta Part A Mol. Biomol. Spectrosc.* 118 (2014) 287–293. <https://doi.org/10.1016/j.saa.2013.08.056>.
- [78] O.S. Rabotyagova, P. Cebe, D.L. Kaplan, Collagen structural hierarchy and susceptibility to degradation by ultraviolet radiation, *Mater. Sci. Eng. C.* 28 (2008) 1420–1429. <https://doi.org/10.1016/j.msec.2008.03.012>.
- [79] J.S. Cobb, V. Zai-Rose, J.J. Correia, A. V Janorkar, FT-IR Spectroscopic Analysis of the Secondary Structures Present during the Desiccation Induced Aggregation of Elastin-Like Polypeptide on Silica, *ACS Omega.* 5 (2020) 8403–8413. <https://doi.org/10.1021/acsomega.0c00271>.

- [80] J. Gaar, R. Naffa, M. Brimble, Enzymatic and non-enzymatic crosslinks found in collagen and elastin and their chemical synthesis, *Org. Chem. Front.* 7 (2020) 2789–2814. <https://doi.org/10.1039/D0QO00624F>.
- [81] E.P. Paschalis, K. Verdellis, S.B. Doty, A.L. Boskey, R. Mendelsohn, M. Yamauchi, Spectroscopic Characterization of Collagen Cross-Links in Bone, *J. Bone Miner. Res.* 16 (2001) 1821–1828. <https://doi.org/10.1359/jbmr.2001.16.10.1821>.
- [82] K.W. Sanden, U. Böcker, R. Ofstad, M.E. Pedersen, V. Høst, N.K. Afseth, S.B. Rønning, N. Pleshko, Characterization of Collagen Structure in Normal, Wooden Breast and Spaghetti Meat Chicken Fillets by FTIR Microspectroscopy and Histology, *Foods.* 10 (2021) 548. <https://doi.org/10.3390/foods10030548>.
- [83] Y. Kolinko, A. Malečková, P. Kochová, M. Grajciarová, T. Blassová, T. Kural, A. Trailin, L. Červenková, J. Havránková, L. Vištejnová, P. Tonarová, V. Moulisová, M. Jiřík, A. Zavaďáková, F. Tichánek, V. Liška, M. Králíčková, K. Witter, Z. Tonar, Using virtual microscopy for the development of sampling strategies in quantitative histology and design-based stereology, *Anat. Histol. Embryol.* 51 (2022) 3–22. <https://doi.org/https://doi.org/10.1111/ahe.12765>.
- [84] V. Howard, M. Reed, *Unbiased Stereology*, Garland Science, 2004. <https://doi.org/10.4324/9780203006399>.
- [85] T. Kural, M. Grajciarová, J. Rosendorf, R. Pálek, L. Červenková, A. Malečková, S. Šarčević, V. Liška, Z. Tonar, Histological mapping of healing of the small and large intestine – A quantitative study in a porcine model, *Ann. Anat. - Anat. Anzeiger.* 249 (2023) 152095. <https://doi.org/https://doi.org/10.1016/j.aanat.2023.152095>.
- [86] P. Tomášek, Z. Tonar, M. Grajciarová, T. Kural, D. Turek, J. Horáková, R. Pálek, L. Eberlová, M. Králíčková, V. Liška, Histological mapping of porcine carotid arteries — An animal model for the assessment of artificial conduits suitable for coronary bypass grafting in humans, *Ann. Anat. - Anat. Anzeiger.* 228 (2020) 151434. <https://doi.org/10.1016/j.aanat.2019.151434>.
- [87] Z. Tonar, T. Kubíková, C. Prior, E. Demjén, V. Liška, M. Králíčková, K. Witter, Segmental and age differences in the elastin network, collagen, and smooth muscle phenotype in the tunica media of the porcine aorta, *Ann. Anat. - Anat. Anzeiger.* 201 (2015) 79–90. <https://doi.org/10.1016/j.aanat.2015.05.005>.
- [88] S. Tschanz, J.P. Schneider, L. Knudsen, Design-based stereology: Planning, volumetry and sampling are crucial steps for a successful study, *Ann. Anat. - Anat. Anzeiger.* 196 (2014) 3–11. <https://doi.org/10.1016/j.aanat.2013.04.011>.
- [89] H.J.G. Gundersen, Notes on the estimation of the numerical density of arbitrary profiles: the edge effect, *J. Microsc.* 111 (1977) 219–223. <https://doi.org/https://doi.org/10.1111/j.1365-2818.1977.tb00062.x>.
- [90] M. Jiřík, Z. Tonar, A. Králíčková, L. Eberlová, H. Mírka, P. Kochová, T. Gregor, P. Hošek, M. Svobodová, E. Rohan, M. Králíčková, V. Liška, Stereological quantification of microvessels using semiautomated evaluation of X-ray microtomography of hepatic vascular corrosion casts, *Int. J. Comput. Assist. Radiol. Surg.* 11 (2016) 1803–1819. <https://doi.org/10.1007/s11548-016-1378-3>.
- [91] A. Malečková, P. Mik, V. Liška, R. Pálek, J. Rosendorf, K. Witter, M. Grajciarová, Z. Tonar, Periphery of porcine hepatic lobes has the smallest length density of hepatic sinusoids and bile canaliculi: A stereological histological study with implications for liver biopsies, *Ann. Anat. - Anat. Anzeiger.* 250 (2023) 152157. <https://doi.org/10.1016/j.aanat.2023.152157>.
- [92] D.S. Kerby, The Simple Difference Formula: An Approach to Teaching Nonparametric Correlation, *Compr. Psychol.* 3 (2014) 11.IT.3.1. <https://doi.org/10.2466/11.IT.3.1>.
- [93] S. Grossman, C. Porth, *Porth's pathophysiology : concepts of altered health states*, Ninth edit, Wolters Kluwer Health/Lippincott Williams & Wilkins, Philadelphia SE, 2014.
- [94] A. Mieczkowska, S.A. Mansur, N. Irwin, P.R. Flatt, D. Chappard, G. Mabileau, Alteration of the bone tissue material properties in type 1 diabetes mellitus: A Fourier transform infrared microspectroscopy study, *Bone.* 76 (2015) 31–39. <https://doi.org/10.1016/j.bone.2015.03.010>.
- [95] X. Ren, H. Shao, Q. Wei, Z. Sun, N. Liu, Advanced Glycation End-products Enhance Calcification in Vascular Smooth Muscle Cells, *J. Int. Med. Res.* 37 (2009) 847–854. <https://doi.org/10.1177/147323000903700329>.
- [96] T. Tanikawa, Y. Okada, R. Tanikawa, Y. Tanaka, Advanced Glycation End Products Induce Calcification of Vascular Smooth Muscle Cells through RAGE/p38 MAPK, *J. Vasc. Res.* 46 (2009) 572–580. <https://doi.org/10.1159/000226225>.
- [97] Q. Wei, X. Ren, Y. Jiang, H. Jin, N. Liu, J. Li, Advanced glycation end products accelerate rat vascular calcification through RAGE/oxidative stress, *BMC Cardiovasc. Disord.* 13 (2013) 13. <https://doi.org/10.1186/1471-2261-13-13>.
- [98] R.K. Dutta, R.B. Roijers, P.H.A. Mutsaers, P. Pauwels, J.J.M. De Goeij, G.J. Van Der Vusse,

- Calcium/phosphorus ratios in calcium-rich deposits in atherosclerotic human coronary arteries, *Nucl. Instruments Methods Phys. Res. Sect. B Beam Interact. with Mater. Atoms.* 231 (2005) 257–262. <https://doi.org/10.1016/j.nimb.2005.01.067>.
- [99] R. Villa-Bellostá, *Vascular Calcification: A Passive Process That Requires Active Inhibition*, Biology (Basel). 13 (2024). <https://doi.org/10.3390/biology13020111>.
- [100] R.V. Bellostá, V. Sorribas, Calcium phosphate deposition with normal phosphate concentration: Role of pyrophosphate, *Circ. J.* 75 (2011) 2705–2710. <https://doi.org/10.1253/circj.CJ-11-0477>.
- [101] R. Villa-Bellostá, *Vascular calcification: Key roles of phosphate and pyrophosphate*, *Int. J. Mol. Sci.* 22 (2021). <https://doi.org/10.3390/ijms222413536>.
- [102] M.J. Thubrikar, *Vascular Mechanics and Pathology*, Springer US, Boston, MA, 2007. <https://doi.org/10.1007/978-0-387-68234-1>.
- [103] D. Wu, Y.H. Shen, L. Russell, J.S. Coselli, S.A. LeMaire, Molecular mechanisms of thoracic aortic dissection, *J. Surg. Res.* 184 (2013) 907–924. <https://doi.org/10.1016/j.jss.2013.06.007>.
- [104] J. Tong, Y. Cheng, G.A. Holzapfel, Mechanical assessment of arterial dissection in health and disease: Advancements and challenges, *J. Biomech.* 49 (2016) 2366–2373. <https://doi.org/10.1016/j.jbiomech.2016.02.009>.
- [105] S. Sherifova and, G.A. Holzapfel, Biochemomechanics of the thoracic aorta in health and disease, *Prog. Biomed. Eng.* 2 (2020) 032002. <https://doi.org/10.1088/2516-1091/ab9a29>.
- [106] Z. Petřivý, L. Horný, P. Tichý, Traction-separation law parameters for the description of age-related changes in the delamination strength of the human descending thoracic aorta, *Biomech. Model. Mechanobiol.* (2024). <https://doi.org/10.1007/s10237-024-01871-1>.
- [107] M.C. Silverstein, K. Bilici, S.W. Morgan, Y. Wang, Y. Zhang, G.S. Boutis, 13 C, 2 H NMR Studies of Structural and Dynamical Modifications of Glucose-Exposed Porcine Aortic Elastin, *Biophys. J.* 108 (2015) 1758–1772. <https://doi.org/10.1016/j.bpj.2015.02.005>.
- [108] A. Gautieri, F.S. Passini, U. Silván, M. Guizar-Sicairos, G. Carimati, P. Volpi, M. Moretti, H. Schoenhuber, A. Redaelli, M. Berli, J.G. Snedeker, Advanced glycation end-products: Mechanics of aged collagen from molecule to tissue, *Matrix Biol.* 59 (2017) 95–108. <https://doi.org/https://doi.org/10.1016/j.matbio.2016.09.001>.
- [109] J. Kamml, C.-Y. Ke, C. Acevedo, D.S. Kammer, The influence of AGEs and enzymatic cross-links on the mechanical properties of collagen fibrils, *J. Mech. Behav. Biomed. Mater.* 143 (2023) 105870. <https://doi.org/https://doi.org/10.1016/j.jmbbm.2023.105870>.
- [110] S. Pal, A. Tsamis, S. Pasta, A. D’Amore, T.G. Gleason, D.A. Vorp, S. Maiti, A mechanistic model on the role of “radially-running” collagen fibers on dissection properties of human ascending thoracic aorta, *J. Biomech.* 47 (2014) 981–988. <https://doi.org/10.1016/j.jbiomech.2014.01.005>.
- [111] X. Shi, Y. Bai, Y. Ke, R. Chen, X. Lin, L. Chen, H. Hong, Ageing-related aorta remodelling and calcification occur earlier and progress more severely in rats with spontaneous hypertension, *Histol. Histopathol.* 33 (2018) 727–736. <https://doi.org/10.14670/HH-11-971>.
- [112] A. Brüel, H. Oxlund, Changes in biomechanical properties, composition of collagen and elastin, and advanced glycation endproducts of the rat aorta in relation to age, *Atherosclerosis.* 127 (1996) 155–165. [https://doi.org/https://doi.org/10.1016/S0021-9150\(96\)05947-3](https://doi.org/https://doi.org/10.1016/S0021-9150(96)05947-3).
- [113] N. Rabbani, P.J. Thornalley, Protein glycation – biomarkers of metabolic dysfunction and early-stage decline in health in the era of precision medicine, *Redox Biol.* 42 (2021) 101920. <https://doi.org/10.1016/j.redox.2021.101920>.
- [114] D. Koole, J.A. van Herwaarden, C.G. Schalkwijk, F.P.J.G. Lafeber, A. Vink, M.B. Smeets, G. Pasterkamp, F.L. Moll, A potential role for glycated cross-links in abdominal aortic aneurysm disease, *J. Vasc. Surg.* 65 (2017) 1493-1503.e3. <https://doi.org/10.1016/j.jvs.2016.04.028>.
- [115] H. Hoshino, M. Takahashi, K. Kushida, T. Ohishi, K. Kawana, T. Inoue, Quantitation of the crosslinks, pyridinoline, deoxypyridinoline and pentosidine, in human aorta with dystrophic calcification, *Atherosclerosis.* 112 (1995) 39–46. [https://doi.org/10.1016/0021-9150\(94\)05395-Y](https://doi.org/10.1016/0021-9150(94)05395-Y).
- [116] D. Skovgaard, R.B. Svensson, J. Scheijen, P. Eliasson, P. Mogensen, A.M.F. Hag, M. Kjær, C.G. Schalkwijk, P. Schjerling, S.P. Magnusson, C. Couppe, An advanced glycation endproduct (AGE)-rich diet promotes accumulation of AGEs in Achilles tendon, *Physiol. Rep.* 5 (2017). <https://doi.org/10.14814/phy2.13215>.
- [117] G.E. Hein, M. Köhler, P. Oelzner, G. Stein, S. Franke, The advanced glycation end product pentosidine correlates to IL-6 and other relevant inflammatory markers in rheumatoid arthritis, *Rheumatol. Int.* 26 (2005) 137–141. <https://doi.org/10.1007/s00296-004-0518-1>.
- [118] M. Kalousová, L. Novotny, T. Zima, M. Braun, L. Vitek, Decreased levels of advanced glycation end-

- products in patients with Gilbert syndrome., *Cell. Mol. Biol. (Noisy-Le-Grand)*. 51 (2005) 387–392.
- [119] D. Wågsäter, V. Paloschi, R. Hanemaaijer, K. Hultenby, R.A. Bank, A. Franco-Cereceda, J.H.N. Lindeman, P. Eriksson, Impaired Collagen Biosynthesis and Cross-linking in Aorta of Patients With Bicuspid Aortic Valve, *J. Am. Heart Assoc.* 2 (2013). <https://doi.org/10.1161/JAHA.112.000034>.
- [120] J.C. -Y. Chung, E. Wong, M. Tang, D. Eliathamby, T.L. Forbes, J. Butany, C.A. Simmons, M. Ouzounian, Biomechanics of Aortic Dissection: A Comparison of Aortas Associated With Bicuspid and Tricuspid Aortic Valves, *J. Am. Heart Assoc.* 9 (2020). <https://doi.org/10.1161/JAHA.120.016715>.
- [121] H.I. Michelena, A.D. Khanna, D. Mahoney, E. Margaryan, Y. Topilsky, R.M. Suri, B. Eidem, W.D. Edwards, T.M. Sundt, M. Enriquez-Sarano, Incidence of Aortic Complications in Patients With Bicuspid Aortic Valves, *JAMA*. 306 (2011) 1104. <https://doi.org/10.1001/jama.2011.1286>.
- [122] F.S. Cikach, C.D. Koch, T.J. Mead, J. Galatioto, B.B. Willard, K.B. Emerton, M.J. Eagleton, E.H. Blackstone, F. Ramirez, E.E. Roselli, S.S. Apte, Massive aggrecan and versican accumulation in thoracic aortic aneurysm and dissection, *JCI Insight*. 3 (2018). <https://doi.org/10.1172/jci.insight.97167>.
- [123] K. Janda, M. Krzanowski, M. Gajda, P. Dumnicka, E. Jasek, D. Fedak, A. Pietrzycka, M. Kuźniewski, J.A. Litwin, W. Sułowicz, Vascular Effects of Advanced Glycation End-Products: Content of Immunohistochemically Detected AGEs in Radial Artery Samples as a Predictor for Arterial Calcification and Cardiovascular Risk in Asymptomatic Patients with Chronic Kidney Disease, *Dis. Markers*. 2015 (2015) 153978. <https://doi.org/https://doi.org/10.1155/2015/153978>.
- [124] S.Y. Yu, H.T. Blumenthal, The Calcification of Elastic Fibers. I. *Biochemical Studies*, *J. Gerontol.* 18 (1963) 119–126. <https://doi.org/10.1093/geronj/18.2.119>.
- [125] J. Atkinson, Age-related medial elastocalcinosis in arteries: mechanisms, animal models, and physiological consequences, *J. Appl. Physiol.* 105 (2008) 1643–1651. <https://doi.org/10.1152/jappphysiol.90476.2008>.
- [126] S. V Dorozhkin, *Calcium Orthophosphates: Applications in Nature, Biology, and Medicine*, Jenny Stanford Publishing, 2012. <https://doi.org/10.1201/b12312>.
- [127] N. Eliaz, N. Metoki, Calcium phosphate bioceramics: A review of their history, structure, properties, coating technologies and biomedical applications, *Materials (Basel)*. 10 (2017). <https://doi.org/10.3390/ma10040334>.
- [128] G.A. Holzapfel, R.W. Ogden, Constitutive modelling of arteries, *Proc. R. Soc. A Math. Phys. Eng. Sci.* 466 (2010) 1551–1597. <https://doi.org/10.1098/rspa.2010.0058>.
- [129] G.A. Holzapfel, J.A. Niestrawska, R.W. Ogden, A.J. Reinisch, A.J. Schriefl, Modelling non-symmetric collagen fibre dispersion in arterial walls, *J. R. Soc. Interface*. 12 (2015) 20150188. <https://doi.org/10.1098/rsif.2015.0188>.
- [130] J.D. Humphrey, G.A. Holzapfel, Mechanics, mechanobiology, and modeling of human abdominal aorta and aneurysms, *J. Biomech.* 45 (2012) 805–814. <https://doi.org/https://doi.org/10.1016/j.jbiomech.2011.11.021>.
- [131] M. Latorre, J.D. Humphrey, A mechanobiologically equilibrated constrained mixture model for growth and remodeling of soft tissues, *ZAMM - J. Appl. Math. Mech. / Zeitschrift Für Angew. Math. Und Mech.* 98 (2018) 2048–2071. <https://doi.org/10.1002/zamm.201700302>.
- [132] A. Rachev, T. Shazly, A structure-based constitutive model of arterial tissue considering individual natural configurations of elastin and collagen, *J. Mech. Behav. Biomed. Mater.* 90 (2019) 61–72. <https://doi.org/10.1016/j.jmbbm.2018.09.047>.